How *Vibrio cholerae* Type VI Secretion System Blocks Intestinal Epithelial Repair

By

Xinyue Xu

A thesis submitted in partial fulfillment of the requirements for the degree of

Master of Science

In

Immunology

Department of Medical Microbiology and Immunology

University of Alberta

Abstract

To maintain an effective barrier, intestinal epithelial progenitor cells must divide at a rate that matches the loss of dead and dying cells. Epithelial damage during most enteric infection accelerates cell proliferation and tissue repair via multiple stress responses. However, infection with the causative agent of cholera, *Vibrio cholerae*, blocks the proliferation of intestinal progenitor cells in a Type VI Secretion System (T6SS)-dependent manner and therefore arrests epithelial repair in the *Drosophila* infection model, which exacerbates diarrheal disease symptoms and shortens host lifespan. It is unknown how *V. cholerae* circumvents such a critical antibacterial defense. Previously, our lab found that *V. cholerae* T6SS enhances transcriptional expression of multiple Bone Morphogenetic Protein (BMP) pathway components in the fly progenitor compartment. We consider this discovery noteworthy, as BMP members of the Transforming Growth Factor-β (TGF-β) cytokine family regulate intestinal homeostasis in flies and vertebrates. In both systems, BMPs act in a paracrine manner to inhibit progenitor proliferation and promote intestinal epithelial cell differentiation. At present, molecular mechanisms of how *V. cholerae* T6SS arrest host tissue repair remain unclear. We consider this an important question, as failure to repair damage in intestinal epithelium exposes the host to lumenal microbes, increasing the risk of systemic infection and chronic inflammation.

Using *Drosophila*, I demonstrated that *V. cholerae* infection activates the BMP signaling specifically in intestinal progenitors in a T6SS-dependent manner. As the T6SS mediates interactions with gut-resident bacteria, I examined the contribution of gut commensals to T6SS-responsive BMP activation. In germ-free flies without gut microbiome, *V. cholerae* infection failed to induce BMP response in progenitors or block progenitor

growth, indicating that BMP activation requires pathogen-commensal interactions. Next, I asked if host innate immune response is involved in regulating BMP activity during *V. cholerae* infection. Loss of the immune deficiency (IMD) protein ablated progenitor-specific BMP response. Furthermore, the enterocyte-specific Relish, an NF-κB family transcription factor in the IMD pathway, is essential for BMP activation during *V. cholerae* infection. Then, I tested if progenitor-specific BMP activation is necessary to block epithelial repair upon infection. Without BMP activity, *V. cholerae* infection could no longer limit progenitor proliferation. Mechanistically, BMP in enteroblasts of the progenitor compartment suppresses intestinal stem cell proliferation non cell autonomously. Finally, I asked if the impacts of *V. cholerae* T6SS on intestinal epithelial renewal apply to vertebrate hosts. Using the zebrafish model, I found that *V. cholerae* T6SS promotes damage, blocks proliferation, and induces TGF-β/BMP activation in the intestine, indicating an evolutionarily conserved link between infection, BMP, and failure in tissue repair. Combined, the findings in this thesis highlight how pathogen-commensal interactions engage host immune response and growth regulatory pathways to disrupt intestinal epithelial repair.

Preface

This thesis contains original work from Xinyue Xu that is in preprint form, sent to Cell Reports, and currently under revision. Dr. Edan Foley was the supervisory author involved in concept formation and manuscript composition:

- **Xu, X.** and Foley, E. *Vibrio cholerae* Arrests Intestinal Epithelial Proliferation through T6SS-dependent Activation of the Bone Morphogenetic Protein Pathway. *Cell Reports* (Under Revision). *Biorxiv*. **doi**: https://doi.org/10.1101/2023.06.29.547108. Data from this manuscript are shown in Chapter 3 Figures 3.1-3.3, Figures 3.5 & 3.6, Figures 3.8-3.10, Figure 3.11C-F, and Figure 3.12.

Dedication

Dedicated to all the minority scholars in STEM.

Acknowledgment

Throughout the course of this M.Sc., my life has been enriched and inspired in so many ways by numerous people. First, I am immensely grateful to my supervisor Dr. Edan Foley. Thank you for being such an amazing person. Thank you for your always open door (allowing me to ask my "two questions" every time), continuous support, and invaluable mentorship. I deeply appreciate your passion for science and have enjoyed all of our conversations about science and life. I will be forever grateful to you for creating a supportive and inclusive environment and your consideration of women and other minority scholars. I have been extremely lucky to have the opportunity to study in your lab, and I hope to pass on that kind of enrichment I received from you to the next generation of students. Wish you all the very best.

Thanks to all the past and present Foley lab members for your tremendous support and friendship over the years. Special thanks to Dr. Meghan Ferguson and Dr. Minjeong Shin for guiding me and showing me how amazing flies are when I first joined the lab. Another huge thanks to our technician Lena Jones for all your efforts and dedication in making everything run so smoothly in the lab. I would also like to thank my best friends Mckenna Eklund and Ralph Derrick V. Graham for all the mental support, field trips, and amazing singing and dancing (love you)! To our Postdoc Aurélia Joly, thanks for the intellectual conversations about flies and life, merci beaucoup. Thanks to Dr. Reegan Willms for all your support and inspiration, and I wish you great joy in your new career life. To all current undergraduate students, Alisha Duggal, Keltie Stewart, and Tim Garcia, it is such a pleasure to study with you. Wish you the best of luck in your future. Vive la Flish!

Huge thanks to my committee members Dr. Maya Shmulevitz and Dr. Robert Ingham for always being supportive and for all the valuable suggestions and discussions about my thesis project.

I am also grateful for all the technical support from numerous core facilities at the University of Alberta. Thank you to microscopy support from Dr. Steven Ogg, Gregory Plummer, and Kiera Smith at Cell Imaging Core, transmission electron microscopy support from Sara Amidian and Dr. Xuejun Sun at the Department of Oncology Cell Imaging Facility, immunohistochemistry support provided by Dr. Kacie Norton at the Department of

Biological Sciences Advanced Microscopy, and flow cytometry support from Dr. Aja Rieger, Lai Xu, and Rikus Niemand at Flow Cytometry Facility. I would also like to thank Science Animal Support Services and the Alberta Health Sciences Animal Laboratory Services for their excellent care of the zebrafish aquatic facilities.

Thank you to the current and past members of the MMI department. I had the privilege of being surrounded by amazing students, staff, and faculties. Special shout out to Tabitha Nguyen and Debbie Doudiet for your dedication, tremendous support, and for always caring about students' wellbeing. Thank you!

Finally, I am forever grateful to my family and friends. Special thanks to my parents Zonghui Wu and Shihong Xu who have always loved me and supported my every choice. Although we live in different countries, you are always there when I need to talk, being willing to hear all the stories, happy or sad, about my life. Thank you, and I love you so much. Thank you to my friends for all the time we spent together, playing badminton, hiking, or chatting. The thesis would not have been possible without you.

Financial support for this project is from the Alberta Graduate Excellence Scholarship and Li Ka Shing Institute of Virology Graduate Studies Entrance Award.

Table of Contents

Chapter 2. Materials and Methods

Chapter 3. *Vibrio cholerae* Arrests Intestinal Epithelial Proliferation through T6SS-dependent Activation of the Bone Morphogenetic Protein Pathway

List of Tables

List of Abbreviations

Chapter 2. Materials and Methods

List of Figures

Chapter 1. Introduction

Chapter 3. *Vibrio cholerae* Arrests Intestinal Epithelial Proliferation through T6SS-dependent Activation of the Bone Morphogenetic Protein Pathway

Chapter 4. Discussion

List of Abbreviations

Arm	Armadillo
BMP	Bone morphogenetic protein
CR	Conventionally reared
CTX	Cholera toxin
DAP-PGN	Diaminopimelic acid-type peptidoglycan
Dl	Delta
Dpp	Decapentaplegic
DSS	Dextran sodium sulfate
EB	Enteroblast
EC	Enterocyte
Ecc15	*Erwinia carotovora carotovora*, isolate 15
EE	Enteroendocrine cell
EGFR	Epidermal growth factor receptor
Esg	escargot
GF	Germ-free
GFP	Green fluorescent protein
IBD	Inflammatory bowel disease
IEC	Intestinal epithelial cell
IMD	Immune deficiency
ISC	Intestinal stem cell
JAK-STAT	Janus kinase/signal transducer and activator of transcription
JNK	Jun N-terminal kinase
LB	Lysogeny broth
MAD	Mother against Dpp

MARTX	Multifunctional autoprocessing repeats-in-toxin
MRS	De Man, Rogosa and Sharpe
MyoIA	MyosinIA
NF-κB	Nuclear Factor of kappa light polypeptide gene enhancer in B-cells
PAAR	Proline-alanine-alanine-arginine
PBS	Phosphate buffered saline
PCNA	Proliferating cell nuclear antigen
PGN	Peptidoglycan
PGRP	Peptidoglycan recognition protein
PH3	Phospho-histone H3
PM	Peritrophic matrix
Pros	Prospero
PVP-I	Polyvinylpyrrolidone-iodine
Rel	Relish
Shn	Schnurri
Su(H)	Suppressor-of-hairless
T6SS	Type VI secretion system
TCP	Toxin coregulated pilus
TGF-β	Transforming Growth Factor-β
Tkv	Thickveins
TNFR	Tumor necrosis factor receptor
UAS	Upstream Activating Sequence
V. cholerae	*Vibrio cholerae*

Table 1.0 *Drosophila* genetics nomenclature

Notation	**Type**	**Example**
Comma (,)	Genes within a chromosome	*esg-Gal4, tub-Gal80^{ts}, UAS-GFP*
Forward slash (/)	Genes on homologous chromosomes	*Su(H)GBE-GAL4,UAS-GFP/CyO*
Semi colon (;)	Genes on heterologous chromosomes	*w;Myo1A-GAL4/CyO;tubGAL80^{ts},UAS-GFP/TM6B*
Plus (+)	Wild-type chromosome	*esg^{ts}/+*
Greater than (>)	Expression with the GAL4 UAS system	*esg^{ts}>shn^{RNAi}*

Chapter 1

Introduction

1.1 The intestinal epithelium

1.1.1 The *Drosophila* intestine

Gut anatomy: The gut of vinegar fly, *Drosophila melanogaster,* shares fundamental similarities with the human gastrointestinal tract in both structure and function, which makes it a useful model for studying intestinal homeostasis and disease. The fly gut comprises three different domains, namely the foregut, midgut, and hindgut (1). The foregut contains the crop for storing food, pharynx, and esophagus. The cardia located at the foregut/midgut junction regulates food passage into the midgut. The midgut is the largest part and the main site of digestion and absorption, which is divided into five regions (R1-R5) with distinct morphology and function (2). The anterior midgut (R1 and R2) is enriched in enzymes for the processing of lipids and proteins (2). The middle midgut (R3) contains copper cells that secrete acid, which are functionally comparable to the vertebrate gastric parietal cells (3). The posterior midgut (R4 and R5) is highly proliferative and functionally analogous to the mammalian small intestine. Similar to the human large intestine, the hindgut regulates absorption of water and ions and controls the passage of gut content out of the body (4).

Intestinal epithelial cell composition: The fly gut is a pseudostratified epithelium composed of cell types equivalent to the vertebrate intestine. In both fly and vertebrate, multipotent intestinal stem cells (ISCs) proliferate and differentiate to self-renew and generate transient cell types that further mature into absorptive and secretory lineages (Figures 1.1 A-D)(2,5–10). In the fly gut, ISCs express the Notch ligand Delta and generate a post-mitotic transient cell type enteroblast (EBs) (Figures 1.1C and 1.1F). ISCs and EBs are collectively referred to as intestinal progenitor cells, characterized by expression of transcription factor *escargot* (*esg*) (Figures 1.1E and 1.1F). EBs express the transcription factor *Suppressor-of-hairless* (*Su(H)*) and further differentiate into *MyosinIA* (*MyoIA*)-expressing absorptive enterocytes (ECs), which undergo several rounds of endoduplication to achieve the characteristic polyploid nuclei and large size (Figures 1.1E and 1.1F). Large columnar ECs make up ~70% of the epithelial cells and extend an apical microvilli brush border to facilitate nutrient uptake. Secretory enteroendocrine (EE) cells express the neuro-endocrine marker Prospero (Pros) and secrete peptide hormones and digestive enzymes

into distal tissues and lumen (Figure 1.1E)(11). A chitinous layer called the peritrophic matrix functions similarly to vertebrate mucus to protect intestinal epithelial cells from environmental insults (Figure 1.1D)(12). Moreover, the fly midgut is surrounded by visceral muscles, serving as a dynamic niche and secreting ligands of multiple signaling pathways, which are essential to epithelial cell functions (13–16).

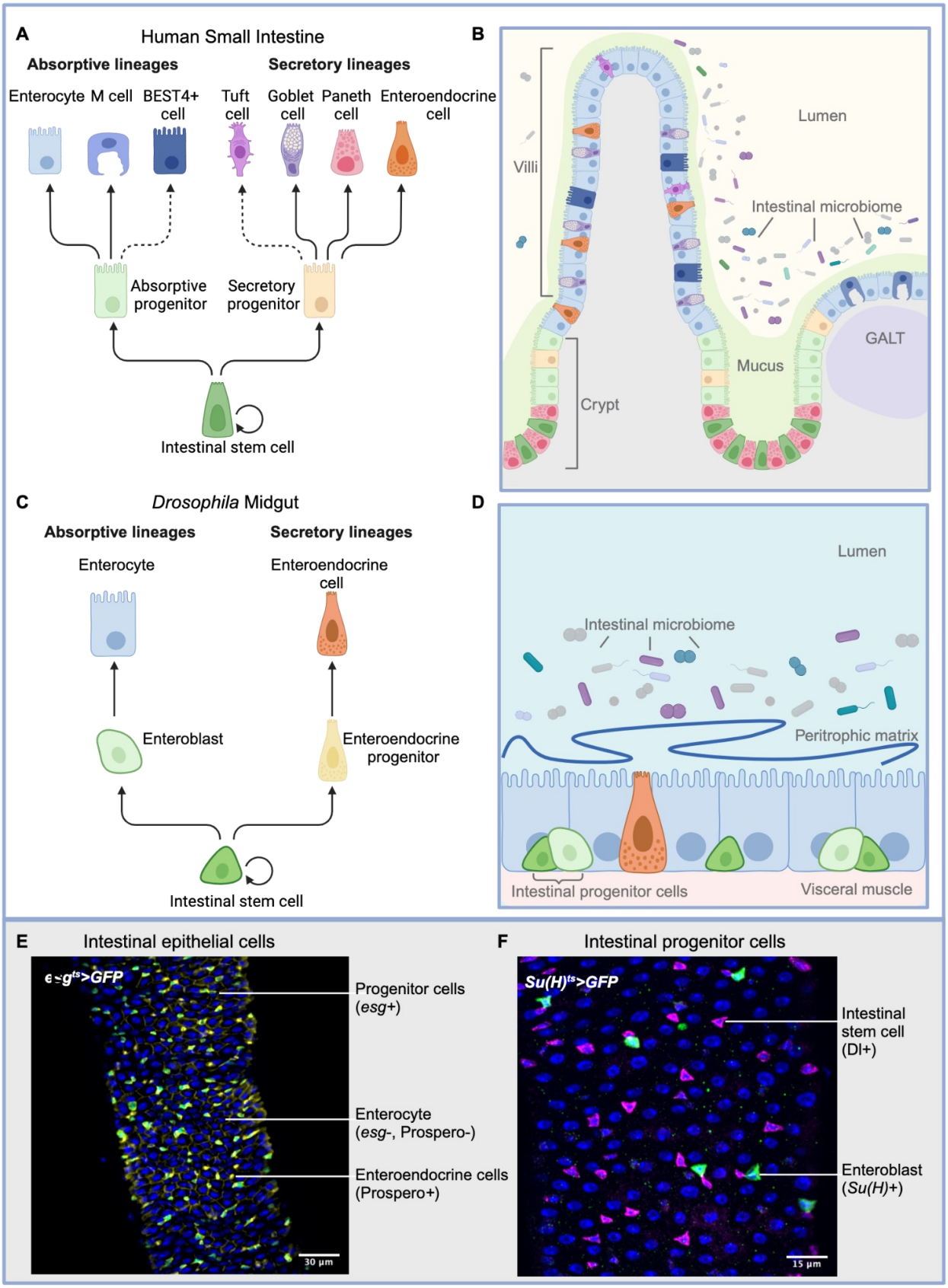
A
Human Small Intestine
Absorptive lineages
Secretory lineages
Enterocyte
M cell
BEST4+ cell
Tuft cell
Goblet cell
Paneth cell
Enteroendocrine cell
Absorptive progenitor
Secretory progenitor
Intestinal stem cell
B
Villi
Lumen
Intestinal microbiome
GALT
Mucus
Crypt
C
Drosophila Midgut
Absorptive lineages
Secretory lineages
Enterocyte
Enteroendocrine cell
Enteroblast
Enteroendocrine progenitor
Intestinal stem cell
D
Lumen
Intestinal microbiome
Peritrophic matrix
Intestinal progenitor cells
Visceral muscle
E
Intestinal epithelial cells
esg^ts>GFP
Progenitor cells (esg+)
Enterocyte (esg-, Prospero-)
Enteroendocrine cells (Prospero+)
30 µm
F
Intestinal progenitor cells
Su(H)^ts>GFP
Intestinal stem cell (Dl+)
Enteroblast (Su(H)+)
15 µm

Figure 1.1 Comparison of intestinal epithelial structure and cellular composition in humans and *Drosophila*. (A) The human intestinal epithelial cells differentiated from intestinal stem cells that give rise to progenitors, which further mature into different absorptive and secretory lineages. Dashed arrows indicate tentative lineages. **(B)** The human small intestine is organized into villi and crypts, possesses gut-associated lymphoid tissue (GALT), and limits microbial contact with a mucus layer. **(C)** The *Drosophila* intestinal stem cell generates an absorptive and a secretory lineage. **(D)** The intestinal epithelium in the fly is a pseudostratified monolayer that limits contact with microbes with the peritrophic matrix. **(E)** Immunofluorescence image of posterior midgut of adult female esg^{ts} fly. esg^{ts}*>GFP* marks intestinal progenitor cells (green), Prospero and Armadillo mark enteroendocrine cells and cell borders, respectively (yellow), and Hoechst marks nuclei (blue). **(F)** immunofluorescence image of posterior midgut of adult female $Su(H)^{ts}$ fly. $Su(H)^{ts}$*>GFP* marks enteroblasts (green), Delta (Dl) marks intestinal stem cells (magenta), and DNA is stained by Hoechst (blue).

The immune deficiency pathway: The intestinal epithelium constantly interacts with a variety of microbes. Therefore, the host develops immune defenses in the gut to tolerate commensals and eliminate pathogens. Unlike vertebrates, flies lack an adaptive immune system, and antibacterial defenses in the gut are primarily mediated by the Immune Deficiency (IMD) pathway. IMD pathway mediates production of antimicrobial peptides and shares extensive similarities to the vertebrate Tumor Necrosis Factor Receptor (TNFR) signaling (Figure 1.2)(17,18). The IMD response is activated by the recognition of the bacterial cell wall component, diaminopimelic acid (DAP) type peptidoglycan (PGN). Once bound to DAP-PGN, PGN recognition protein (PGRP) receptors dimerize and recruit a signaling complex composed of the adaptor protein IMD, FADD, and caspase DREDD (19,20). Cleavage of the IMD by DREDD induces activation of TAK1 and subsequent IKK complex activation (21). IKK in turn phosphorylates the *Rel*/NF-κB transcription factor Relish, which allows DREDD-mediated cleavage and nuclear translocation of the N-terminal NF-κB-like domain to initiate transcription of antimicrobial peptides (22–24). TAK1 also induces activation of c-Jun N-Terminal Kinase (JNK) signaling that is mainly involved in stress response and cytoskeletal rearrangement (25). Besides the bactericidal role of IMD, recent

work uncovered cell type-specific roles for the IMD NF-κB axis in intestinal homeostasis, including regulation of epithelial cell proliferation and differentiation (26,27). For instance, progenitor-specific IMD activity promotes the maturation of the secretory lineage (26,28). In addition, activation of IMD during enteric infection promotes delamination of damaged epithelial cells, blocks ISC proliferation, and effectively prevents barrier repair in infected hosts (29–31). Together, these results demonstrate that IMD response is essential for maintaining the intestinal barrier under a homeostatic condition or during infection.

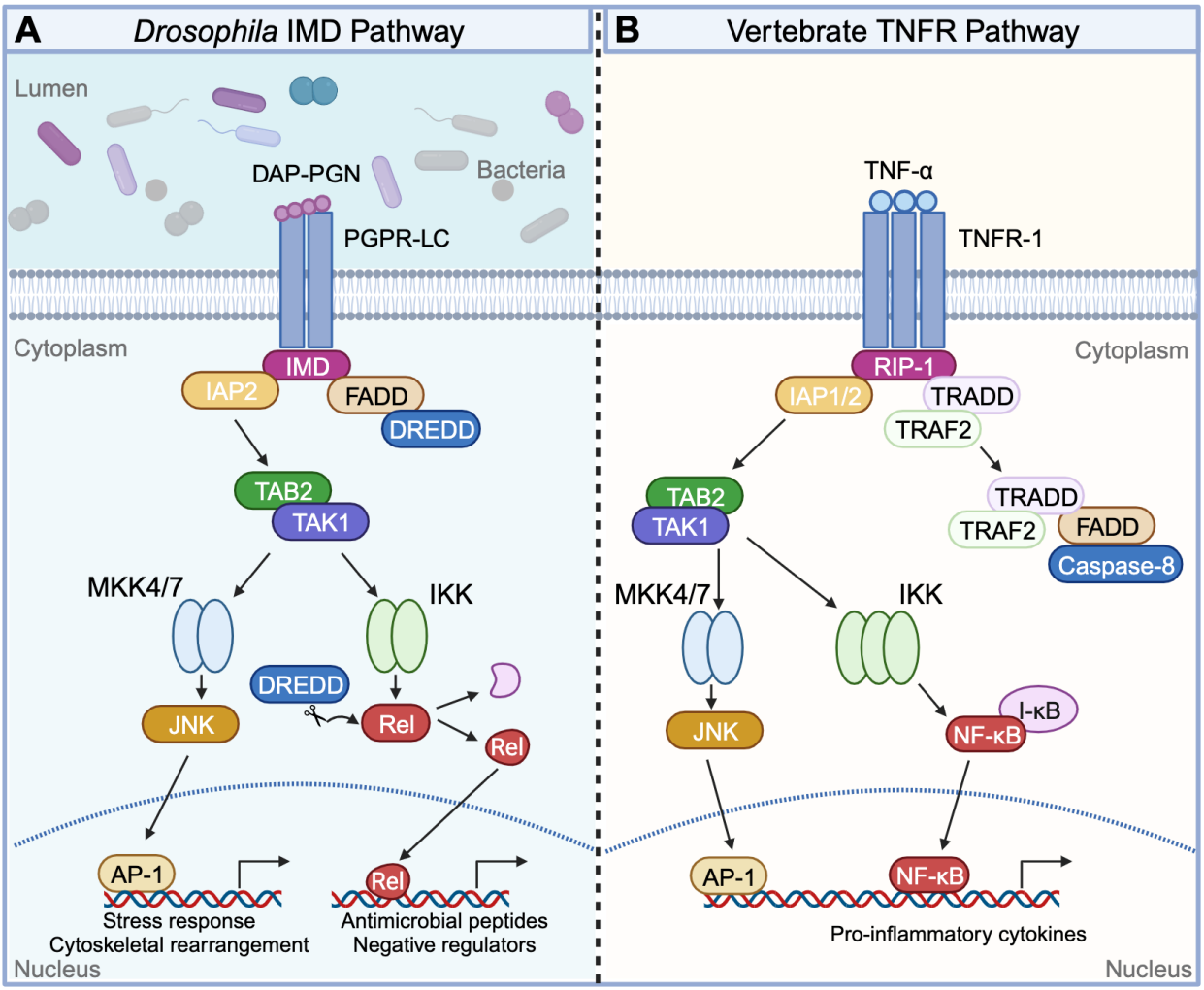

Figure 1.2 The *Drosophila* Immune Deficiency (IMD) pathway and vertebrate Tumor Necrosis Factor Receptor (TNFR) pathway. Schematic representations of the **(A)** fly IMD pathway and **(B)** vertebrate TNFR signaling. Orthologous proteins between fly and vertebrate are identified by the same colors and shapes. Abbreviations in the IMD pathway:

DAP-PGN, diaminopimelic acid-type peptidoglycan; PGRP-LC, peptidoglycan recognition protein LC; FADD Fas-associated death domain; DREDD, death related ced-3/Nedd2-like caspase; IAP2, inhibitor of apoptosis 2; TAB2, TAK1-associated binding protein 2; TAK1, TGF-beta activated kinase 1; IKK, I-**κ**B kinase; MKK4/7, MAP kinase kinase 4/7; JNK, c-Jun N-terminal kinase; AP-1, adaptor protein complex 1; Rel, Relish. Abbreviations in the TNFR pathway: RIP-1, receptor interacting protein 1; TRADD, tumor necrosis factor receptor type 1-associated DEATH domain protein; TRAF2, TNF receptor-associated factor 2; I-**κ**B, inhibitor of **κ**B; NF-**κ**B, nuclear factor-**κ**B.

1.1.2 Intestinal epithelial repair

To maintain an effective barrier against harmful environmental agents, multipotent ISCs divide at a pace that matches the loss of dying epithelial cells. For example, infectious microbes frequently damage the epithelium, which induces host defenses that prompt the expulsion of damaged cells (32–35). In response, ISCs divide at an accelerated rate to ensure an adequate supply of mature cells to maintain barrier integrity. Epithelial repair by ISCs is regulated by a diverse network of evolutionarily conserved signaling pathways in both flies and vertebrates. On one hand, stress and growth responses including epidermal growth factor receptor (EGFR), Janus kinase/signal transducer and activator of transcription (JAK-STAT), and JNK pathways promote ISC proliferation (14,15,36–40). Diffusible EGF ligands secreted from damaged ECs, visceral muscles, and progenitors activate the EGFR pathway in ISCs to induce cell mitosis (14,15,36). Similarly, Unpaired 2 and 3 produced by ECs initiate JAK-STAT signaling in ISCs to promote cell division and facilitate epithelial repair (37). On the other hand, negative regulators like Hippo and Bone Morphogenetic Protein (BMP) signalings play a pivotal role in balancing ISC proliferation, which prevents uncontrolled cell growth and malignant transformation upon epithelial damage (41,42).

Impaired epithelial renewal abates barrier function, allowing lumenal microbes to invade interstitial tissue, and promote disease (34,43). Thus, it is essential that we understand the molecular mechanisms that regulate epithelial repair during enteric infections.

1.2 The Bone Morphogenetic Protein (BMP) signaling in the intestine

1.2.1 The BMP/SMAD pathway

BMPs are morphogens belonging to the transforming growth factor β (TGF- β) superfamily, which were first identified as factors critical for bone and cartilage formation. Now BMPs are well known to be essential for a wide array of biological functions, including dorsal-ventral patterning, regulation of immune responses, and development and homeostasis of gastrointestinal organs (44–46). The BMP signaling pathway is conserved and ubiquitous in animals. Compared with vertebrates, fewer representatives of each signaling component are present in *Drosophila*, which simplifies the mechanistic study of the BMP pathway (47). In both fly and vertebrates, activation of canonical BMP/SMAD signaling begins with binding of BMP ligands to a heteromeric receptor complex composed of two type I and two type II transmembrane serine-threonine kinases. The active type II receptor then phosphorylates the GS domain within the type I receptor, which in turn recruits and activates receptor-activated SMAD (R-SMAD) by phosphorylation. Phosphorylated R-SMAD then forms a complex with common SMAD (co-SMAD), and this SMAD complex translocates to the nucleus where it regulates gene expression with a variety of cofactors. In *Drosophila*, mother against decapentaplegic (MAD) is the primary R-SMAD that transduces all BMP signals with the co-SMAD Medea and cofactor Schnurri (47).

1.2.2 BMP signaling in intestinal development

Gut looping: Looping of the initially straight embryonic gut tube maximizes the absorptive capacity of the gut by extending the gut length well beyond the linear length of the organism while permitting proper placement of the lengthy intestine within the body cavity. Throughout development, the gut tube remains attached to the body wall by the dorsal mesentery. As these two tissues grow at different rates, the elongation of the gut tube against the constraint of the dorsal mesentery generates mechanical forces that drive looping (48). A recent study showed that BMP signaling directly modulates gut looping in the chicken embryo. Specifically, BMP ligand BMP2 enriched in the dorsal mesentery activates BMP signaling and suppresses mesentery growth, which establishes differential elongation rates between the gut and mesentery, generating compressive forces that bend

the intestine into loops (49). Furthermore, BMP activity in the small intestine directly regulates the tightness of loops. Overexpression of BMP2 leads to tightly coiled loops, whereas overexpression of BMP pathway inhibitor Noggin reduces coiling in the gut (49).

Villus morphogenesis: Villi are a regular array of finger-like projections extended into the intestinal lumen, allowing for nutrient absorption, digestion, secretion, and immune responses. BMP signaling coordinates with the Hedgehog (Hh) pathway to induce villi formation and development. In the mammalian intestine, villi arise as domes over condensed clusters of mesenchymal cells (50). Epithelial Hh signaling plays a critical role in the emergence and aggregation of the mesenchymal clusters (51). The newly formed clusters dynamically express multiple BMP ligands (BMP2, BMP4, BMP5, BMP7) and BMP pathway modifiers (Twsg1, Noggin, Fstl1) (52). In the intestine explant, increasing BMP ligand concentration inhibits cluster formation, whereas a complete BMP signaling inhibition induces formation of two to three times larger and fused clusters. Consistent with *ex vivo* findings, depletion of Type I BMP receptors in Hh-responsive mesenchymal cells results in larger clusters and wide villi *in vivo*. Collectively, these results suggest that BMP signaling controls distribution and patterning of villus clusters (52).

Intestinal epithelial cell differentiation: BMP signaling is essential for terminal differentiation of multiple intestinal epithelial cell lineages. In *Drosophila*, BMP plays an important role in specification of copper cells, which secrete acids to maintain the low lumenal pH in the copper cell region of middle midgut (3). Overexpressing BMP ligand decapentaplegic (*dpp*) significantly increases the number of copper cells and induces an expansion of the copper cell region from the middle midgut into the anterior midgut. Conversely, blocking BMP signaling in the copper cell region leads to a complete loss of functional copper cells (16,53). In the mammalian intestine, BMP is essential for maturation of secretory cell precursors. Compared to wild-type mice, *Bmpr1a* mutant mice show a more than two-fold decrease in expression of factors regulating terminal differentiation of goblet cells (54). Moreover, loss of intestinal epithelial BMP signaling leads to a significant decrease in enteroendocrine cell number by 75% per crypt-villus axis (54). A recent study suggested that canonical BMP signaling also regulates terminal differentiation of the absorptive cell lineage. Individual BMPs derived from sub-epithelial mesenchymal cells activate distinct

differentiation programs in ECs, specifying EC precursors into villus tip or villus center mature ECs (55).

Intestinal epithelial cell proliferation: BMP signaling represents one of the most important counterforces that limits ISC expansion and, therefore, prevents hyperproliferation of the intestinal epithelium. Mammalian ISCs reside basally in crypts as two populations, slowly cycling, damage-resistant +4 ISCs and actively cycling columnar cells specified by the expression of Wnt target gene Lgr5 (56). A recent study determined that BMP restricts $Lgr5^+$ ISC self-renew. Deletion of BMP type I receptor Bmpr1a induces ISC hyperproliferation under homeostatic conditions and accelerates crypt regeneration after irradiation (57). Further studies show that BMP/SMAD signaling directly restricts the stemness of $Lgr5^+$ ISC by repressing the expression of multiple stem cell signature genes, which is mediated by the SMAD recruitment of histone deacetylase 1 to promoters of target genes (57). Recent findings in *Drosophila* also reveal that BMP signaling impacts ISC proliferation through a variety of different mechanisms. One group showed that BMP ligands released from visceral muscle induced by epithelial damage inhibit ISC proliferation by directly activating BMP signaling in ISCs (16). Another group suggested that EC-specific BMP activity limits ISC expansion. Specifically, trachea-derived BMP ligands activate BMP signaling in ECs, which prevents the loss of ECs upon injury. The stabilized ECs in turn suppress ISC proliferation (53). Loss of BMP signaling in EBs induces hyperproliferation of ISCs under normal conditions and upon infection with the entomopathogen *Erwinia carotovora carotovora 15* (*Ecc15*) (58). Given the pivotal role of BMP signaling in maintaining intestinal homeostasis, abnormal BMP activity is related to many intestinal diseases.

1.2.3 BMP signaling in intestinal diseases

Juvenile polyposis syndrome (JPS): JPS is an autosomal dominant disorder with the development of multiple hamartomatous polyps throughout the gastrointestinal tract, which increases the risk of developing colorectal cancer. Loss of function in BMP transcription factor SMAD4 and receptor BMPR1A account for approximately half of all JPS cases (59,60). Mice with overexpression of BMP inhibitor Noggin in the intestinal epithelium develop JPS-like phenotypes, including generation of new crypts, branching villi, dilated cysts filled with mucin, and an increase in inflammatory cells (61). In another study, inactivation of *bmpr1a*

in both intestinal epithelium and mesenchyme triggers an expansion of ISC and progenitor populations, which eventually results in polyp growth and elevated inflammation in the intestine, resembling human JPS (42). In contrast, deletion of *bmpr1a* solely in intestinal epithelium did not induce polyp formation in mice (42). In *Drosophila*, loss of MAD, a homolog of vertebrate SMAD4, from visceral muscle underneath epithelial cells results in hyperplasia and tumor growth, similar to those described for JPS (16). These findings suggest a non-cell autonomous pathological mechanism of JPS in which BMP activity in surrounding tissues participates in tumor suppression.

Inflammatory bowel diseases (IBDs): IBDs including ulcerative colitis and Crohn's disease are intestinal disorders characterized by chronic relapsing inflammation. Several studies have shown that BMPs play critical roles in IBD pathogenesis. BMP6 regulates iron metabolism in the intestine by controlling the expression of hepcidin (62,63). Anemia in IBD patients is associated with an increased hepcidin level that lowers serum iron (64). Anti-BMP6 reagents inhibit hepcidin expression, increase serum iron levels, and alleviate intestinal inflammation in DSS-induced colitis mice (65). In rats with trinitrobenzenesulfonic (TNBS)-induced IBD, systematic administration of BMP7 significantly reduces expression of pro-inflammatory cytokines, prevents intestinal fibrosis, and limits colitis formation (66). Moreover, expression of BMP antagonists such as Grem1 and Noggin is elevated during IBD (66,67). Interestingly, BMP7 therapy reduces Noggin levels in TNBS-induced colitis tissues (66). These findings collectively indicate that BMP pathway components, especially BMP7 and BMP antagonists, have therapeutic potential for patients with IBD.

1.3 *Vibrio cholerae* disease and the type VI secretion system

1.3.1 Cholera

V. cholerae: V. cholerae, a Gram-negative bacterium belonging to the phylum Proteobacteria and the family *Vibrionaceae*, is the causative agent of the disease cholera. This bacterium is characterized by its curved rod shape with a polar flagellum for motility (68). In the environment, *V. cholerae* inhabits estuarine and coastal water and exists as a free-living bacterium or forms a biofilm on a number of abiotic and biotic surfaces (69). Algae, copepods, shellfish, insects and fish are natural reservoirs for *V. cholerae* (70–74). The

prevalence of these organisms contributes to the spread of the bacteria in endemic regions during seasonal flooding.

The disease cholera: Cholera is caused by ingestion of *V. cholerae* contaminated water or food and subsequent intestinal colonization by the pathogens. There are an estimated three million cholera cases with 100,000 deaths annually in endemic regions around 50 countries (75,76). Symptoms of cholera range from mild gastrointestinal distress to fatal diarrhea. Severe cholera cases are marked by up to one liter per hour of purged "rice-water" stool with water, salt, mucus, and live pathogens (77). The diarrhea results in severe electrolyte loss and dehydration, which then causes hypovolemia, hypoglycemia, hypotonic shock, and eventually leads to renal and heart failure (78). Currently, the seventh pandemic affects a wide region of our planet. Normally, rehydration and treatment with electrolytes can reduce mortality rates from 50-70% to 0.5% (78). However, the disease is most likely to affect people in areas impacted by conflicts and natural disasters, due to the lack of clean water and accessible health infrastructures. From 2016 to 2018, the Yemeni civil war alone resulted in the worst cholera outbreak in modern history with over one million suspected cases (79). Furthermore, while antibiotics and vaccines protect from *V. cholerae* infection, antibiotic-resistant strains are emerging, and current vaccines provide moderate and time-limited protection (80). Therefore, it is essential that we develop a complete molecular profile of the gut response to *V. cholerae* infection.

V. cholerae in cholera pandemics: Over more than 200 serotypes, only O1 *V. cholerae* has been implicated in cholera pandemics. O1 *V. cholerae* are further divided into two subgroups, classical O1 strains and El Tor strains. Classical O1 *V. cholerae* is hypothesized to be responsible for the first six pandemics, which causes a more violent and brief disease, characterized by the production of cholera toxin. El Tor strains cause the ongoing seventh pandemic, trending into a milder and more prolonged disease course (81–83). Recent studies revealed genotypic and phenotypic differences between these two sets of strains. The cholera toxin protein CtxB differs by two amino acids between the classical and El Tor variants (84). Moreover, differences in the toxin coregulated pilus (tcp) P and tcpH promoter significantly reduce cholera toxin production in El Tor strains (84,85). El Tor *V. cholera* also encodes a number of auxiliary virulence factors, including a multifunctional autoprocessing repeats-in-toxin (MARTX) toxin, zinc metalloprotease hemagglutinin, a pore-forming

hemolysin, and a function type VI secretion system (T6SS), which are not encoded by classical *V. cholerae* and may contribute to pathogenicity differences between these two variants (86–88).

1.3.2 The *Vibrio cholerae* type VI secretion system

Structure and assembly of the T6SS: The T6SS is a syringe-like protein apparatus used by over a quarter of Gram-negative bacteria to deliver toxic effectors into a variety of prokaryotic and eukaryotic cells (89). The T6SS is composed of a membrane complex, a baseplate, an outer sheath, and an inner tube loaded with effectors, which extends from the cytoplasm to the outer membrane, homologous to the T4 bacteriophage tail and spike (Figure 1.3)(90). Assembly of the T6SS begins with the membrane complex composed of VasD, VasF, and VasK, which spans the bacterial inner membrane to provide structural support to the system (Figure 1.3A)(91). *V. cholerae* with mutation in membrane complex proteins cannot assemble the T6SS (T6SS-deficient)(92). Next, the baseplate starts to form in the cytoplasm, which is then recruited by the membrane complex and anchored to the inner membrane, serving as the construction site of the tail complex (91,93,94). The tail complex contains the inner tube formed by hemolysin coregulated protein hexamer encased within an outer sheath made of VipA and VipB proteins (91,93,94). VgrG protein trimer forms the tip of the inner tube, and proteins containing repeating proline-alanine-alanine-arginine (PAAR) cap the VgrG trimer to sharpen the T6SS spike complex (91,93). VipA/B outer sheath continues to grow until it contacts the inner membrane at the other end of the cell (95). In response to uncharacterized signals, a rapid contraction of the outer sheath propels the inner tube into the extracellular space, which punctures the membrane of the target prey to deliver toxic effectors (Figure 1.3B)(96,97).

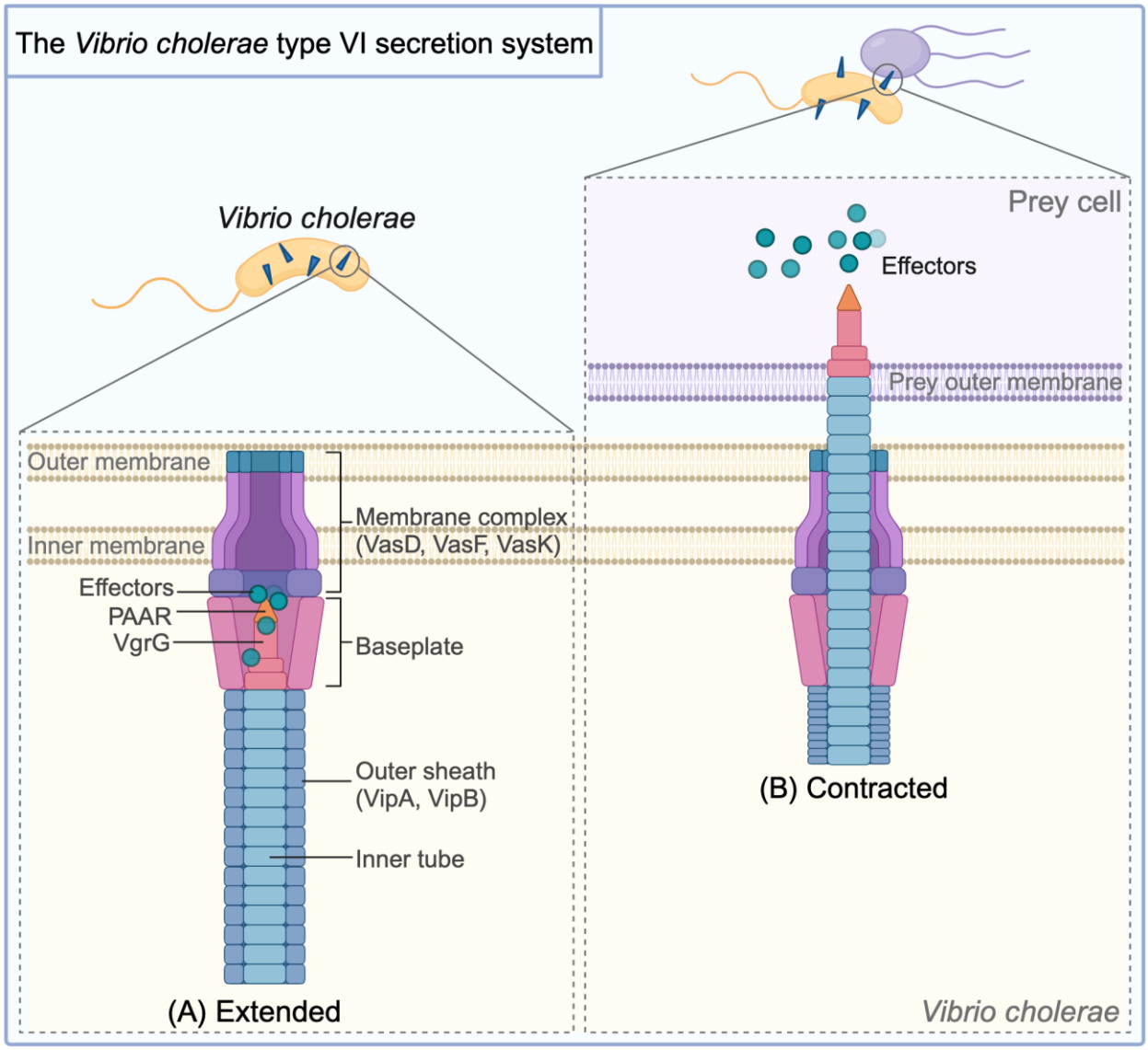

Figure 1.3 The *Vibrio cholerae* T6SS. Schematic representation of the **(A)** extended T6SS that is assembled inside the bacterium and the **(B)** contracted T6SS that delivers effectors into a target prey.

T6SS effectors: Unlike the structure of the T6SS which is highly conserved, functions of T6SS effectors greatly vary among bacterial species and strains. All *V. cholerae* T6SS effectors are either loaded onto the VgrG tip or are part of the tip proteins themselves (98). Moreover, *V. cholerae* encodes immunity proteins that bind and sequester incoming effectors to protect themselves from these toxins (99,100). Pandemic *V. cholerae* strains secret five different effectors: TseL, TseH, and VgrG3 target bacteria (100–102), VgrG1 targets

eukaryotic cells (103), and VasX targets both prokaryotic and eukaryotic cells (92). Antibacterial effectors target conserved cellular components in Gram-negative bacteria. The tip structural protein VgrG3 degrades peptidoglycan in the bacterial cell wall (102). TseL and TseH with lipase and amidase activity, respectively, are loaded onto the tip and secreted (98,100,101). Another structural protein VgrG1 targets eukaryotic cells by actin crosslinking, which has been shown to kill amoeba and macrophages (103,104). VasX targets both prokaryotic and eukaryotic cells by inducing pore formation in the membranes (105). Collectively, *V. cholerae* T6SS effectors target a variety of prey, enhancing bacterial survival in nature and promoting intestinal colonization in a host.

V. cholerae T6SS in the host: V. cholerae infection initiates with colonization of the host intestinal epithelium, where the pathogens form microcolonies and start to produce other virulence factors including cholera toxin. The anti-eukaryotic T6SS effector VgrG1 promotes *V. cholerae* colonization in the infant mouse gut and zebrafish intestine (106,107). Specifically, the actin-crosslinking domain increases contraction of the zebrafish intestine, which expels commensal *Aeromonas veronii* and therefore allows *V. cholerae* to colonize the gut epithelium (107). In addition to targeting host cells, *V. cholerae* uses T6SS to directly outcompete other gut microbes for access to the host. T6SS-dependent killing of commensal *Escherichia coli* in the infant mouse significantly increases *V. cholerae* number and production of virulence factors including cholera toxin in the intestine (108). A recent study from our lab showed that T6SS-symbiont interactions impairs epithelial repair in *Drosophila* intestines upon *V. cholerae* infection (30). Moreover, inactivation of the T6SS or removal of gut commensals restores epithelial renewal, attenuates intestinal damage, and extends the host lifespan after infection (30,106,108,109). Collectively, these findings indicate that T6SS-host-commensal interactions contribute to *V. cholerae* virulence. However, the underlying molecular mechanisms of T6SS-dependent pathogenesis remain unclear, and appropriate animal models are needed to answer these questions.

1.4 Animal models of *Vibrio cholerae* infection

1.4.1 Mammalian models

The infant mouse model: The infant mouse has been used to identify the majority of *V. cholerae* virulence factors such as the lipopolysaccharide O-antigen and toxin hemagglutinin (110). Studies in the infant mouse also revealed that the *V. cholerae* toxin coregulated pilus (TCP) is essential for initial colonization in the intestine (111). A more recent study using this model has shown the importance of T6SS to *V. cholerae* pathogenesis *in vivo*, mainly focusing on the anti-eukaryotic effectors (108). Although studies in the infant mouse have greatly advanced our knowledge about *V. cholerae* infection, this model has several limitations. First, *V. cholerae* infection in infant mice is asymptomatic, and, most importantly, they do not develop the hallmark pathogen-laden diarrhea (112). Additionally, mice become naturally immune to *V. cholerae* when they are five days old, so it can only be used to study the effects of an acute but not long-term infection (113). Also, the infant mouse intestine has an immature adaptive immune system and an underdeveloped microbiome, which hinders the study of pathogen-host-commensal interactions (114).

The adult mouse model: The adult mouse model allows the study of auxiliary virulence factors that appear to have no effect on infant mice. In adult mice, the three auxiliary toxins including the MARTX toxin, a zinc metalloprotease hemagglutinin and a pore-forming hemolysin toxin only encoded by pandemic El Tor *V. cholerae* are essential for prolonged colonization in the gut (115). The fully developed immune system in adult mice also allows the study of immune responses upon infection. Neutrophils were found to clear colonizing *V. cholerae* and reduce systemic inflammation in murine guts (116). The adult mouse model has a number of disadvantages. Like infant mice, adult mice do not develop disease symptoms upon *V. cholerae* infection. Moreover, the traditional virulence factors, cholera toxin and TCP, which cause disease in humans are dispensable for *V. cholerae* pathogenesis in adult mice (115). Furthermore, manipulation of the microbiome is required prior to *V. cholerae* infection, which prevents study of interactions between the pathogen and natural gut symbionts.

The infant rabbit model: Compared to mice, the infant rabbit better models the disease cholera by developing symptoms such as severe diarrhea and body weight loss upon *V.*

cholerae infection (117). Unlike in adult mice, cholera toxin and TCP contribute to bacterial colonization and disease symptoms in the infant rabbit (117). While a powerful model, infant rabbits have several disadvantages. First, the protocol for *V. cholerae* infection is difficult. In order to permit *V. cholerae* colonization in the intestine, the infant rabbit model needs to be pretreated with cimetidine to inhibit stomach acid production (117). Like the infant mouse model, infant rabbits cannot be used to study the long-term infection dynamics due to the development of immunity against *V. cholerae.* Study of pathogen-commensal interactions is also not an option, since the microbiome in infant rabbits is underdeveloped.

1.4.2 The zebrafish model

Zebrafish *Danio rerio* has emerged as a powerful vertebrate model to study *V. cholerae* pathogenesis, which has a number of advantages over traditional mammalian models. First, zebrafish are naturally colonized by *Vibrio* species and contribute to the spread of pathogenic *V. cholerae* in the wild. *V. cholerae* infection in zebrafish is simply adding the bacteria into tank water without any need for pre-treatment (118). Also, infected fish develop a cholera-like disease hallmarked by activation of host immune responses and pathogen-laden diarrhea (119–122). Like the mammalian intestine, the zebrafish gut epithelium contains a complex community of secretory and absorptive cell lineages that interact with immune-regulatory myeloid and lymphoid cells (123–126). Evolutionarily conserved signaling pathways regulate development and cell function in fish and mammalian intestines. Recent studies using the zebrafish model showed that the production of auxiliary toxins promotes intestinal colonization of pandemic El Tor strains (118). Another study in zebrafish demonstrated that T6SS increases *V. cholerae* colonization by inducing intestinal expulsion of commensal bacteria (107). Furthermore, similar to the adult mouse model, the major human *V. cholerae* virulence factors, TCP and cholera toxin, are not required for zebrafish colonization, indicating an alternative mechanism of pathogenesis (118).

1.4.3 The vinegar fly model

The vinegar fly, *Drosophila melanogaster,* is a powerful system to study *V. cholerae* pathogenesis (127). Insects are natural *V. cholerae* reservoirs and contribute to pathogen

dissemination in endemic areas (71,72). Therefore, the protocol for *V. cholerae* is relatively simple in flies, which works by feeding flies *V. cholerae* culture during infection (128). Flies infected with *V. cholerae* develop cholera-like symptoms that include epithelial breaches and watery diarrhea laden with live pathogens (29,30,128). Like vertebrates, loss of cholera toxin does not completely abolish *V. cholerae* virulence in flies, indicating that cholera toxin-independent mechanisms contribute to pathogenesis (29,128,129). Although flies lack an adaptive immune system, it has an intestinal innate immune system analogous to that in vertebrates. For instance, the IMD pathway (29,31), the primary mediator of gut antibacterial defenses, shares extensive similarities to the vertebrate TNFR response (17,18). Furthermore, the presence of a well-characterized commensal population in the fly guts makes it possible to study *V. cholerae*-commensal interactions during induction.

Flies have provided particularly valuable insights into the actions of *V. cholerae* virulence factors. For example, polysaccharide-dependent biofilm formation allows *V. cholerae* to colonize and persist in the fly gut (130). The CtxA component of cholera toxin disrupts enterocyte junctions, leading to leakage, weight loss, and reduced viability (131). Furthermore, infection with *V. cholerae* activates the fly IMD pathway (29,31). *V. cholerae*-dependent activation of IMD contributes to pathogenesis by blocking ISC proliferation and promoting delamination of damaged epithelial cells, effectively preventing barrier repair in infected hosts (29–31). Recent studies using the fly model showed that T6SS-dependent killing of commensal bacteria contributes to *V. cholerae* virulence, as inactivation of the T6SS or removal of gut commensals restores epithelial renewal, attenuates intestinal damage, and extends host lifespan after infection (30,106,108,109). Previously, our lab found that *V. cholerae* enhances transcriptional expression of multiple BMP pathway components in the fly progenitor compartment in a T6SS-dependent manner (30). However, the underlying molecular mechanism of T6SS-dependent arrest of epithelial repair remains unclear.

1.5 Thesis objectives

Enteric infection causes epithelial cell death, which normally accelerates stem cell proliferation to repair damaged tissue and maintain intestinal barrier integrity. In contrast, infection with *V. cholerae* blocks intestinal proliferation in a T6SS-dependent manner (30). It is unknown how *V. cholerae* T6SS arrests epithelial repair. We consider this an important question, as failure to renew the intestinal epithelium exposes peri-intestinal tissue to gut microbes, greatly increasing the risk of systemic infection.

In my thesis project, I aimed to answer this question (Figure 1.4). Our lab previously discovered that *V. cholerae* T6SS significantly enhances the expression of multiple BMP pathway components in *Drosophila* intestinal progenitor cells (30). Typically, activation of BMP signaling in the intestine inhibits cell proliferation. These observations together lead to my hypothesis that *V. cholerae* T6SS-mediated activation of host BMP responses in progenitors blocks proliferation and, therefore, impairs intestinal epithelial repair. Using the *Drosophila* model, I asked how *V. cholerae* infection activates progenitor-specific BMP. Specifically, I determined the role of gut commensals and host innate immune response, IMD pathway, in BMP activation. I also tested if BMP activity is essential to arrest epithelial repair upon *V. cholerae* infection. Furthermore, I used a vertebrate model zebrafish to ask if the impacts of *V. cholerae* T6SS on intestinal epithelial renewal apply to vertebrate hosts. Given the importance of intestinal epithelial barrier function, it is essential that we understand how the interactions between pathogen, host, and commensals affect tissue repair upon enteric infections.

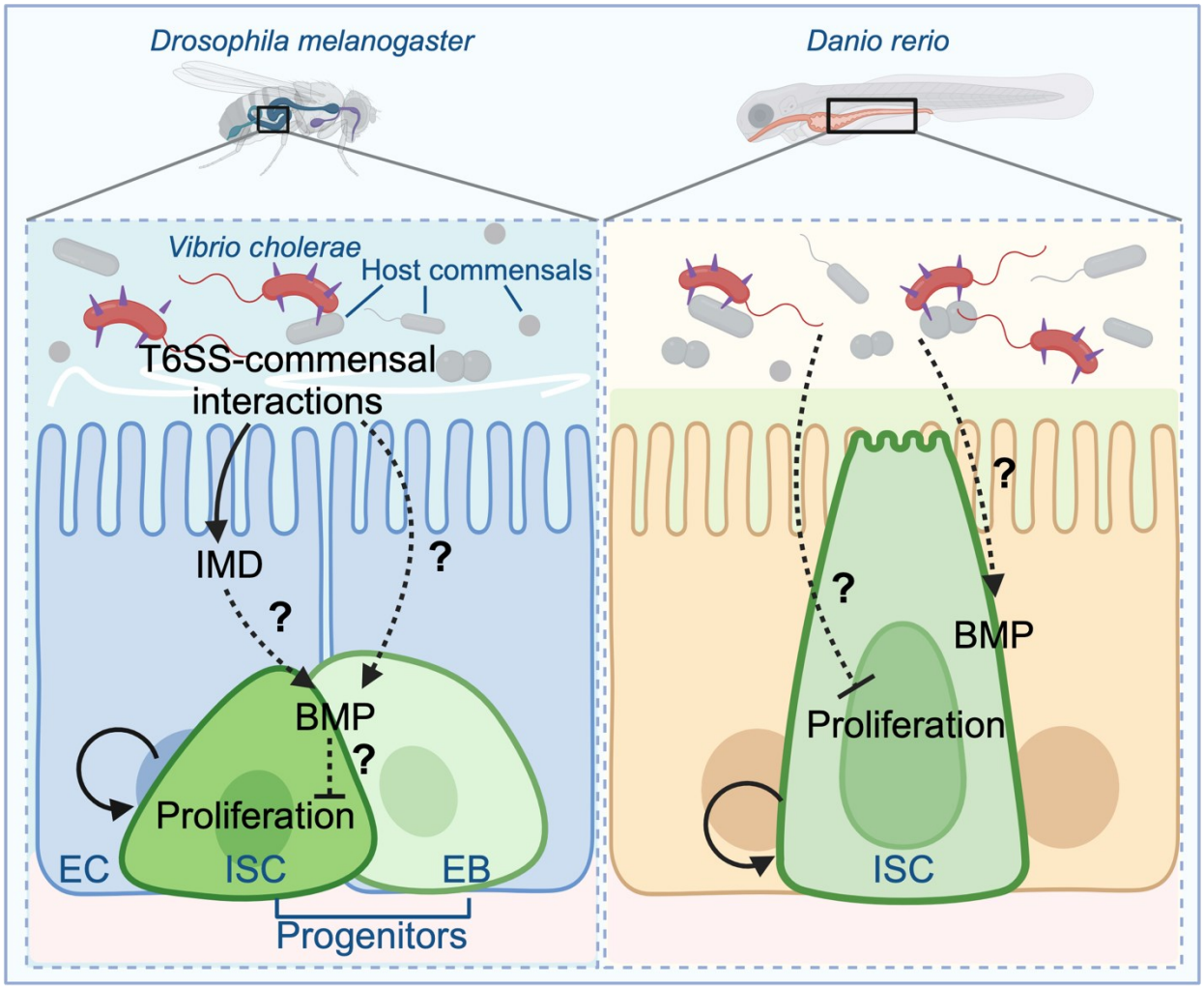

Figure 1.4 Thesis objectives. How does *V. cholerae* infection activate progenitor-specific BMP? Does BMP activation require T6SS-commensal interactions and IMD activity? Is *V. cholerae*-responsive BMP activation essential to arrest epithelial repair? Does the impact of the *V. cholerae* T6SS on intestinal epithelial renewal apply to both invertebrate and vertebrate hosts?

Chapter 2

Materials and Methods

This chapter contains content from the following source:

- **Xu, X.** and Foley, E. *Vibrio cholerae* Arrests Intestinal Epithelial Proliferation through T6SS-dependent Activation of the Bone Morphogenetic Protein Pathway. *Cell Reports* (Under Revision). *Biorxiv*.

  doi: https://doi.org/10.1101/2023.06.29.547108

2.1 Fly and zebrafish husbandry

2.1.1 Fly stocks and handling

Drosophila stocks and crosses were maintained at 18-20°C on a standard cornmeal medium (Nutri-Fly Bloomington formulation; Genesee Scientific). All experimental flies were virgin females. Once 25-30 newly eclosed flies were obtained in each vial, flies were shifted to an incubator with the appropriate temperature (25°C or 29°C) with a 12-hour/12-hour light/dark cycle. Fly lines used in this thesis are as follows:

Table 2.1 Fly lines used in this study

Name	Genotype	Source
esg^{ts} (5)	*w;esg-GAL4,tubGAL80^{ts},UAS-GFP*	Bruce Edgar
Foley *w^{1118}* stock (wild type)	*w^{1118}*	Foley Lab
Foley w stock (wild type)	w	Foley Lab
imd-/- (132)	*y,w, P{EPgy2}imd^{EY08573}*	BDSC (#17474)
Myo1A^{ts}	*w;Myo1A-GAL4/CyO;tubGAL80^{ts},UAS-GFP/TM6B*	Bruce Edgar
Relish RNAi	*UAS-rel^{RNAi}*	VDRC (#49413)
Shn RNAi	*UAS-shn^{RNAi}*	VDRC (#KK-105643)
Su(H)^{ts}	*w;Su(H)GBE-GAL4,UAS-GFP/CyO;ubi-GAL80^{ts}/TM6B*	Bruce Edgar
Tkv CA	*UAS-tkv^{CA}/TM3*	BDSC (#36536)
40D-UAS (Control for VDRC KK lines)	*40D-UAS*	VDRC (#60101)

BDSC (Bloomington *Drosophila* Stock Centre); VDRC (Vienna Drosophila Resource Center)

The conditional expression of cell type-specific transgenes was performed with the temperature-sensitive GAL4/upstream activating sequence (UAS) system. At any temperature equal to or below 25°C, binding of GAL4 to UAS was prevented by $GAL80^{ts}$. At 29°C, inactivation of $GAL80^{ts}$ permits GAL4 activation of transgenes under the control of UAS. Therefore, flies were kept at 18-20°C and shifted to 29°C for 7 days prior to experiments to restrict transgene expression.

In this study, Foley Lab w^{1118} line was used as a wild-type control to set up crosses with esg^{ts} and $Su(H)^{ts}$ lines. The *imd-/-* line was backcrossed into our wild-type w^{1118} background for ten generations prior to use. As *white* (*w*) mutants showed impaired biological functions including stress response in flies (133), we generated a wild-type control, Foley w stock, in Figure 3.6 (WT) for *imd-/-* by introducing the *w+* allele from *Oregon R* line into our w^{1118} via backcrossing for eight generations.

2.1.2 Generation of germ-free flies

To generate germ-free (GF) flies, freshly eclosed female $esg^{ts}/+$ flies were raised on autoclaved food with antibiotics (100µg/mL Ampicillin, 100µg/mL Metronidazole, 50µg/mL Vancomycin dissolved in 50% ethanol, and 100µg/mL Neomycin dissolved in water) for 5 days at 25°C. To ensure sterility, two flies from each vial were homogenized in de Man, Rogosa and Sharpe (MRS) broth and plated on MRS agar plates. Flies were considered GF if no visible colonies formed. Conventionally reared (CR) flies were fed autoclaved food without antibiotics for 5 days at 25°C. On day 6, both GF and CR flies were then transferred onto autoclaved food without antibiotics for 7 days at 29°C, flipping onto freshly prepared food every 2 days. The sterility of GF flies was confirmed by plating fly homogenate on MRS plates 1 day prior to *Vibrio cholerae* infection.

2.1.3 Zebrafish husbandry

Zebrafish were raised and maintained following protocols approved by the Animal Care & Use Committees, Biosciences and Health Sciences at the University of Alberta, operating under the guidelines of the Canadian Council of Animal Care. Adult wild-type TL strain zebrafish were reared at the University of Alberta fish facility at 29°C under a 14-hour/10-hour light/dark cycle using standard zebrafish husbandry protocols. Zebrafish

were fasted for 22 hours prior to *V. cholerae* infection. For larval analysis, TL zebrafish embryos were collected from breeding tanks and transferred to glass petri dishes with embryo media (15 mM NaCl, 1 mM $CaCl_2$•$2H_2O$, 1 mM MgSO4•$7H_2O$, 0.7 mM $NaHCO_3$, 0.5 mM KCl, 0.15 mM KH_2PO_4 and 0.05 mM Na_2HPO_4 in MiliQ water). Embryos were raised at 29°C under a 14-hour/10-hour light/dark cycle. 6 day-post-fertilization larvae were used for *V. cholerae* infection.

2.1.4 Generation of germ-free zebrafish

Adult TL zebrafish were bred for less than 60 minutes to minimize exposure to microbes from parents. Embryos were collected, washed, and split into GF or CR cohorts. The GF cohort was kept in sterile EM supplemented with antibiotics (100μg/mL Ampicillin, 5μg/mL Kanamycin, 250ng/mL Amphotericin B, and 5μg/mL Gentamicin), while the CR cohort was kept in EM. Embryos were incubated at 29°C for 4-6 hours and washed every 2 hours with EM or EM plus antibiotics for CR and GF cohorts respectively. Once embryos were at 50% epiboly, the GF cohort was washed three times with sterile EM, and then 2 minutes with 0.1% Polyvinylpyrrolidone-iodine (PVP-I) in EM. Embryos were rinsed three times with EM and then immersed in 0.003% sodium hypochlorite (bleach) solution for 20 minutes. GF embryos were washed three more times and transferred into tissue culture flasks with sterile EM. CR embryos received the same number and duration of washes with sterile EM rather than PVP-I or bleach. GF confirmation was performed at 4 days post fertilization by plating out 100 μL EM from flasks onto TSA plates. Parental tank water and sterile EM were used as positive and negative control respectively, where bacterial growth was confirmed in tank water and absent in sterile EM. GF and CR flasks with bacterial absent and present respectively were used for subsequent analysis.

2.2 Bacterial Culture and Assays

2.2.1 *V. cholerae* oral infection in flies

Virgin female flies were kept at 29°C for 7 days prior to infection. $esg^{ts}>shn^{RNAi}$ flies and their wild-type counterparts ($esg^{ts}/+$) were maintained at 18°C for 7 days and then shifted to 29°C for 3 days to minimize the detrimental effects of prolonged BMP inactivation. For oral infection in flies, El Tor *V. cholerae* C6706 and C6706Δ*vasK* (104) were grown on Lysogeny Broth (LB) plates (0.5% NaCl, 0.5% yeast extract, 1% tryptone, 1.5% agar) supplemented with 100 μg/ml streptomycin (Sigma SLBK5521V) for 16-18 hours at 37°C. To prepare a *V. cholerae* infection culture, single colonies were removed from the plate, suspended in LB broth, and diluted to a final OD600 of 0.125. Flies were starved for 2 hours at 29°C prior to infection. In each vial, 10-15 flies were placed onto one-third of a cotton plug soaked with 3 ml of LB broth (Uninfected) or *V. cholerae* infection culture (C6706 or C6706Δ*vasK*). Vials were kept at 29°C with a 12-hour/12-hour light/ dark cycle for oral infection.

2.2.2 *V. cholerae* oral infection in zebrafish

For *V. cholerae* infection in zebrafish, a single colony of C6706 or C6706Δ*vasK* was suspended in LB broth with 100 μg/ml streptomycin and grown with aeration overnight at 37°C. *V. cholerae* cells were washed twice with PBS and diluted to OD600 of 1. To infect fish larvae, 15-20 larvae (6 days post fertilization) were incubated in each well of a 6-well plate containing 20 μL infection culture (C6706 or C6706Δ*vasK*) or 20 μL PBS (Uninfected) in 4 mL embryo medium. For infection in adult fish, 5 female fish per treatment were incubated in a 400 mL beaker with 1 mL infection culture (C6706 or C6706Δ*vasK*) or 1 mL PBS (Uninfected) in 200 mL filter sterilized fish tank water. Fish were kept in a 29°C incubator with a 14-hour/10-hour light/ dark cycle during infection.

2.3 Imaging

2.3.1 Immunofluorescence

2.3.1.1 Whole gut mounting

Fly intestines were dissected in ice-cold PBS, fixed in 8% formaldehyde in PBS for 20 minutes, washed in PBS with 0.2% Triton-X (PBST) for 30 minutes, and blocked in PBST with 3% bovine serum albumin (BSA) for 1 hour at room temperature. Guts were protected from light during all these processes. Guts were stained overnight at 4°C in PBST + 3% BSA with appropriate primary antibodies (Table 2.2). On the following day, guts were washed in PBST for 30 minutes and stained for 1 hour at room temperature with secondary antibodies and DNA stain in PBST + 3% BSA. Guts were washed in PBST for 30 minutes at room temperature and then in PBS overnight at 4°C.

Zebrafish larvae (6 day-post-fertilization) were infected with C6706 for 24 hours and then incubated in embryo medium with 1% DMSO and 5 mM EdU (Invitrogen C10340) for 8 hours at 29°C. Fish intestines were dissected in PBS and fixed in 4% paraformaldehyde in PBS overnight at 4°C. Guts were washed three times with PBSTx (0.75% TritonX-100 and 0.02% NaN_3 in PBS), blocked for 1 hour in PBSTx + 3% BSA at room temperature, and stained with primary antibodies in blocking buffer overnight at 4°C. Guts were washed with PBSTx and then stained for 1 hour at room temperature with secondary antibodies and nuclear stain, followed by rinse in PBSTx. EdU detection was performed by incubating guts in Click-iT® reaction cocktail (Invitrogen C10340) for 30 minutes at room temperature. Guts were washed in PBSTx followed by extra washing in PBS.

2.3.1.2 TUNEL assay with sections of adult fish intestines

Intestines from adult TL zebrafish were dissected and fixed in BT fixative (0.15 mM $CaCl_2$, 0.1 M PO_4, 4% sucrose, 4% paraformaldehyde in dH_2O) for 48 hours at 4°C. Guts were embedded in paraffin, sectioned into 5 μm slices, and collected on Superfrost Plus slides. Sections were deparaffinized with Neoclear and rehydrated successively with 100% EtOH, 90% EtOH, 70% EtOH, 50% EtOH and distilled water. Antigen unmasking was performed by boiling slides in 0.1 M sodium citrate buffer (pH 6) in a 98°C water bath for 15 minutes. Slides

were washed with PBST (1xPBS + 0.1% Tween-20) for 2 x 2 minutes, blocked with blocking buffer (3% BSA in PBST) for one hour at room temperature, and stained with primary antibody overnight at 4°C. After secondary antibody staining for one hour at room temperature, sections were washed by PBST and incubated with TUNEL reaction mixture for one hour at 37°C. Sections were washed in PBS for 3 x 5 minutes and stained for 10 minutes at room temperature with DNA stain in PBST followed by washing with PBS 3 x 15 minutes.

For all the immunofluorescence experiments, fly and fish intestines (whole gut and sections) were mounted with Flouromount™ (Sigma; F4680) and visualized with a spinning-disk confocal microscope (Olympus IX-81 motorised microscope base with Yokagawa CSU 10 spinning-disk scan-head). Images of fly posterior midguts (R4/5) and entire zebrafish guts were acquired using Perkin Elmer's Volocity software, and all quantifications were performed manually with Fiji (ImageJ) software. PH3+ cells in the entire fly midgut were counted through the eyepiece of the microscope.

Table 2.2 Antibodies and dyes

Antibody/Dye	Concentration	Source
Chicken anti-GFP	1:2000	Invitrogen PA1-9533
Mouse anti-armadillo (extracellular domain)	1:100	DSHB N2 7A1
Mouse anti-Delta	1:100	DSHB C594.9B
Mouse anti-Prospero	1:100	DSHB MR1A
Rabbit anti-PH3	1:1000	Millipore 06-570
Rabbit anti-pSmad3	1:200	Abcam ab52903
Goat anti-chicken 488	1:1000	Invitrogen A11039
Goat anti-rabbit 568	1:1000	Invitrogen A11011

Goat anti-mouse 647	1:1000	Invitrogen A21235
Hoechst 33258	1:1000	Molecular Probes H3569

DSHB: Developmental Studies Hybridoma Bank

2.3.2 Immunohistochemistry

Paraffin-embedded sections of adult TL zebrafish intestine were deparaffinized with Toluene and rehydrated. Antigen unmasking was performed by boiling slides in 0.1 M sodium citrate buffer (pH 6) in a 98°C water bath for 20 minutes. Sections were incubated in 3% hydrogen peroxide, washed with PBSt (0.5% TritonX-100 in PBS), blocked with 10% normal goat serum in PBSt, and incubated with mouse anti-PCNA (1/20000; Sigma P8825) overnight at 4°C in humid chamber. Sections were washed three times with PBSt and incubated in SignalStain® Boost Detection Reagent (HRP, Mouse; CST 8125P) for 30 minutes at room temperature. SignalStain® DAB Chromogen solution (CST 8059) was added onto each section for colorimetric detection. Slides were rinsed and counterstained with ¼-strength hematoxylin. All sections were dehydrated and mounted in Dpx. Images were captured using ZEISS AXIO A1 compound light microscope with SeBaCam 5.1MP camera, and qualifications were done using Fiji software.

2.3.3 Transmission electron microscopy

Fly posterior midguts were cut into 1 mm pieces and immediately placed into fixative (3% paraformaldehyde and 3% glutaraldehyde in 0.1 M cacodylate buffer with 0.1 M $CaCl_2$, pH 7.2). Tissue processing was performed at the Cell Imaging Facility at University of Alberta. The midgut sagittal sections from 5 flies per treatment were visualized using a JEOL 2100 transmission electron microscope.

2.4 Statistical analysis and figure construction

In Chapter 3, all graphs and plots were constructed using R (version 4.1.1) via R-studio (version 2021.09.0-315) with easyGgplot2 (version 1.0.0.9000). All statistical analysis was completed with R. One-way Analysis of Variance (ANOVA) was used to determine the overall statistical difference, a Tukey's test for Honest Significant Differences was used for multiple comparisons, and an unpaired student t-test was used to compare two different groups. Details of the specific test used for each data panel can be found in the tables and figure captions. Statistical significance was set at $p \leq 0.05$. Figures in Chapter 1 and Chapter 4 were generated using BioRender. Figures in Chapter 3 were assembled using Inkscape.

Chapter 3

Vibrio cholerae Arrests Intestinal Epithelial Proliferation through T6SS-dependent Activation of the Bone Morphogenetic Protein Pathway

This chapter contains content from the following source:

- **Xu, X.** and Foley, E. *Vibrio cholerae* Arrests Intestinal Epithelial Proliferation through T6SS-dependent Activation of the Bone Morphogenetic Protein Pathway. *Cell Reports* (Under Revision). *Biorxiv*.

  doi: https://doi.org/10.1101/2023.06.29.547108

3.1 The T6SS Induces BMP Activation in *Drosophila* Intestinal Progenitors.

In contrast to most enteric challenges, *V. cholerae* causes widespread intestinal epithelial cell (IEC) destruction without a compensatory expansion of the progenitor pool (30,31). At present, we do not understand how this pathogen blocks such an essential damage repair response. Recently, our lab showed that *V. cholerae* enhances the expression of multiple BMP pathway components in intestinal progenitor cells in a T6SS-dependent fashion, including the ligand *dpp*, the type-I BMP receptor *tkv*, and the transcriptional target *spalt* (30). As BMP is an evolutionarily conserved tumor suppressor that arrests IEC proliferation in flies and vertebrates (16,53,56,57), I tested the hypothesis that *V. cholerae* prevents intestinal epithelial repair by activating BMP in progenitors.

In preliminary experiments, I used immunofluorescence-based imaging to determine the rostrocaudal distribution of GFP-expressing C6706, an El Tor *V. cholerae* strain that causes the ongoing seventh pandemic, in infected adult *Drosophila* midguts. I defined four levels of colonization that ranged from absent (level I) to extensive, biofilm-like accumulations (level IV, Figure 3.1A). I observed *V. cholerae* distribution throughout the intestine, with prominent accumulations in the posterior midgut (Figure 3.1B), including IEC-associated *V. cholerae* populations that had breached the peritrophic matrix (Figure 3.1C). As the posterior midgut is a region of high tissue turnover during damage (2), and *V. cholerae* accumulates to the greatest extent in the posterior region, I elected to characterize relationships between this pathogen, BMP, and posterior midgut renewal in greater detail.

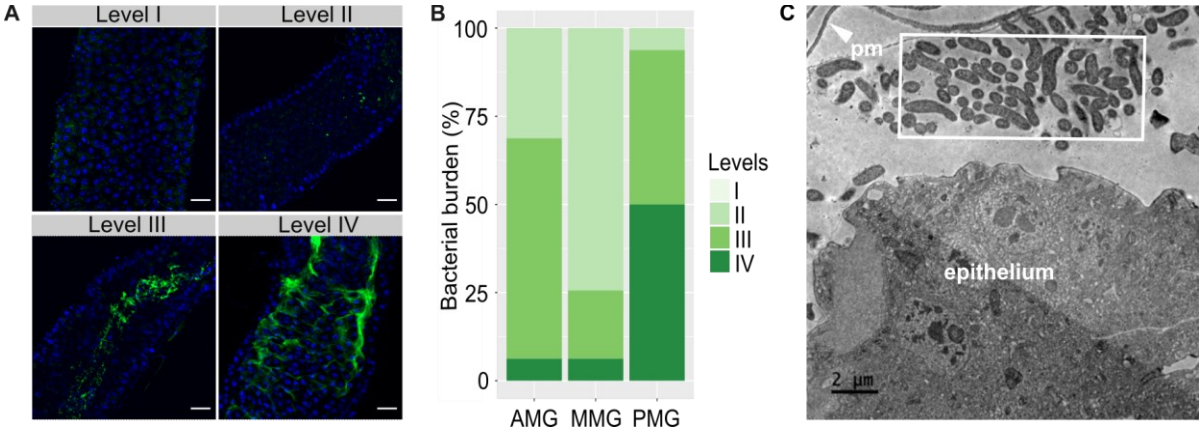

Figure 3.1. *V. cholerae* colonizes the posterior midgut of *Drosophila*.

(A) Immunofluorescence of fly midguts infected with C6706. DNA stained by Hoechst (blue) and GFP-labeled C6706 (green). Four different levels of bacterial burden: level I = no visible GFP-labeled bacteria, level II = a few scattered individual GFP-C6706, and large clumps of *V. cholerae* in the lumen (level III) or in close proximity to the intestinal epithelium (level IV). Scale bars = 25 µm. **(B)** Approximate bacterial burden in different regions of fly guts infected with C6706 (n=20) for 24 h. Assessment based on the four-level scale in (A). Anterior midgut, AMG; middle midgut, MMG; posterior midgut, PMG. **(C)** Transmission electron microscopy of the posterior midguts of flies infected with C6706 for 24 h. Clusters of rod-shaped *V. cholerae* are indicated with a white box. Peritrophic matrix, pm.

To determine if the T6SS activates BMP in host IECs, I quantified MAD phosphorylation (pMAD) in guts of uninfected *esg^{ts}/+* flies, alongside *esg^{ts}/+* flies that were challenged with C6706, or the isogenic T6SS-deficient *vasK* deletion mutant (C6706Δ*vasK*) (104). MAD phosphorylation provides a direct measure of BMP activation in the fly gut, and *esg^{ts}/+* transgenic flies allow us to identify progenitors (small, GFP-positive cells), enteroendocrine cells (Prospero (Pros)-positive and GFP-negative), and enterocytes (large, GFP and Pros-negative cells), effectively allowing us to quantify lineage-specific BMP activation (Figures 1.1E and 3.2A). Regardless of infection status, I observed a high incidence of BMP activation in Pros+ EE cells, indicating *V. cholerae*-independent activation of BMP in the secretory lineage (Figure 3.3). In contrast, I detected substantial, T6SS-specific impacts on BMP activation within the progenitor compartment. Uninfected *esg^{ts}/+* guts contained evenly spaced IECs with minimal BMP activation throughout the epithelium (Figures 3.2A-C). In agreement with earlier reports (30,109), challenges with T6SS-deficient C6706Δ*vasK* disrupted epithelial organization and induced tissue repair with an expansion of the GFP+ progenitor cell compartment (Figures 3.2A and 3.4). I did not observe effects of C6706Δ*vasK* infection on MAD phosphorylation relative to uninfected controls (Figures 3.2A-C), suggesting that T6SS-deficient *V. cholerae* failed to modify the host BMP pathway. Consistent with previous studies (30,31), I found that wild-type *V. cholerae* caused extensive epithelial damage without stimulating progenitor proliferation (Figures 3.2A and 3.4). However, and in contrast to T6SS-deficient C6706Δ*vasK*, the percentage of pMAD+ progenitors almost doubled in C6706-infected guts (Figures 3.2A-C). Combined with our earlier transcriptional profiles (30), our data indicate a T6SS-specific activation of BMP in the progenitor compartment with an accompanying failure to expand progenitor numbers during infection.

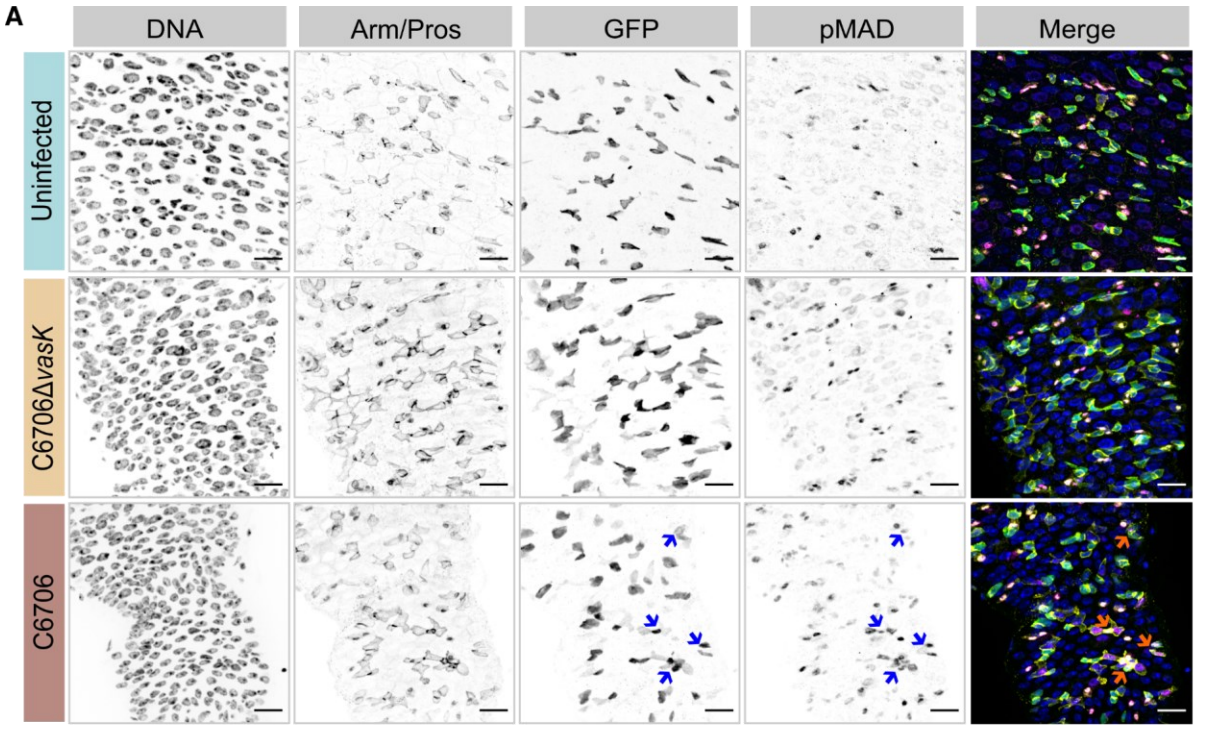

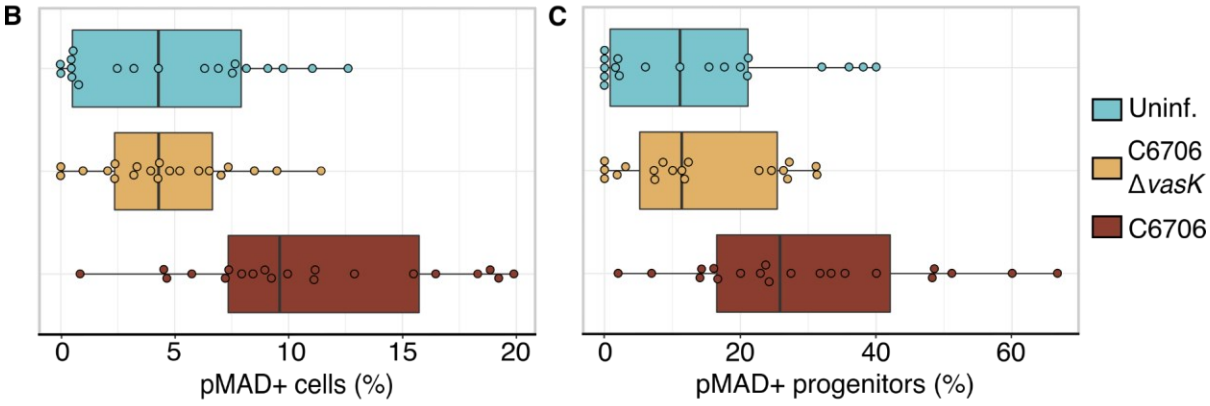

Test	ANOVA	Tukey	
P-value	2.26×10^{-5}	Uninf. vs Δ*vasK*	0.992
		Uninf. vs C6706	2×10^{-4}
		C6706 vs Δ*vasK*	1×10^{-4}

Test	ANOVA	Tukey	
P-value	9×10^{-4}	Uninf. vs Δ*vasK*	1.00
		Uninf. vs C6706	0.003
		C6706 vs Δ*vasK*	0.003

Figure 3.2. *V. cholerae* activates BMP in intestinal progenitor cells in a T6SS-dependent manner. (A) Posterior midguts of *esg^{ts}/+* adult fly uninfected, infected with C6706Δ*vasK* or C6706 for 24 h. Hoechst labels DNA (blue), Armadillo and Prospero (Arm/Pros) label cell borders and enteroendocrine cells, respectively (yellow), GFP labels progenitors (green), and pMAD labels cells with BMP activation (magenta). Arrows = pMAD+ progenitors. Scale bars = 15 μm. **(B and C)** Percentage of **(B)** all cells or **(C)** progenitors that are pMAD+. Each

dot represents a measurement from a single fly gut. P values are calculated using the significance tests indicated in the tables.

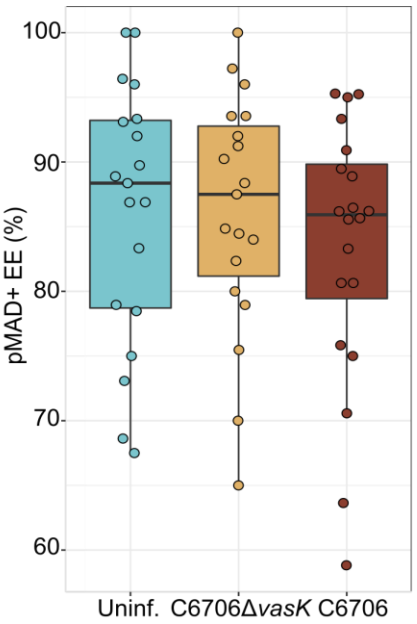

Test	ANOVA	Tukey	
P-value	0.601	Uninf. vs Δ*vasK*	0.999
		Uninf. vs C6706	0.649
		C6706 vs Δ*vasK*	0.669

Figure 3.3. BMP activation in enteroendocrine cells.

Percentage of Pros+ enteroendocrine cells (EE) that are pMAD+ in uninfected *esg*^{ts}/+ guts, and guts infected with C6706Δ*vasK* or C6706. Each dot represents a measurement from a single fly gut. P values were calculated using the significance tests indicated in the table.

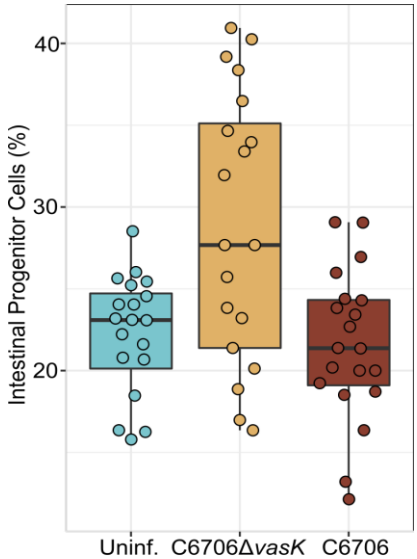

Test	ANOVA	Tukey	
P-value	3.78×10^{-4}	Uninf. vs Δ*vasK*	0.002
		Uninf. vs C6706	0.987
		C6706 vs Δ*vasK*	0.001

Figure 3.4. *V. cholerae* T6SS inhibits expansion of intestinal progenitor compartment.

Percentages of progenitor cells in uninfected, C6706Δ*vasK*-infected or C6706-infected *esg*^{ts}/+ guts. Each dot represents a measurement from a single fly. P values were calculated using the significance tests indicated in the table

3.2 *V. cholerae*-Mediated Activation of BMP Requires Commensal Bacteria and Host Innate Defenses

As T6SS-dependent pathogenesis involves interactions between *V. cholerae* and commensal bacteria in flies and mice (30,108,109), I asked if commensals are also required for T6SS-responsive BMP activation in the gut. In this instance, I quantified infection-dependent BMP activation in germ-free (GF) *esg^{ts}/+* flies relative to conventionally reared (CR) counterparts. I observed a significant increase in pMAD+ progenitor numbers of infected CR flies compared to uninfected controls (Figures 3.5B and 3.5C), with a parallel failure to increase progenitor numbers (Figures 3.5B and 3.5D), further supporting the argument that *V. cholerae* activates BMP while arresting cell proliferation (Figure 3.4). The infected GF guts show clear signs of epithelial damage – loss of neatly organized cell borders, uneven internuclear spacing, and irregular distribution of GFP+ progenitors (Figure 3.5A). However, in the absence of gut resident bacteria, C6706 infection significantly stimulated progenitor expansion (Figures 3.5A and 3.5D), without a progenitor-specific BMP activation (Figures 3.5A and 3.5C), establishing a requirement for gut commensals to support *V. cholerae*-dependent activation of BMP and arrest epithelial repair.

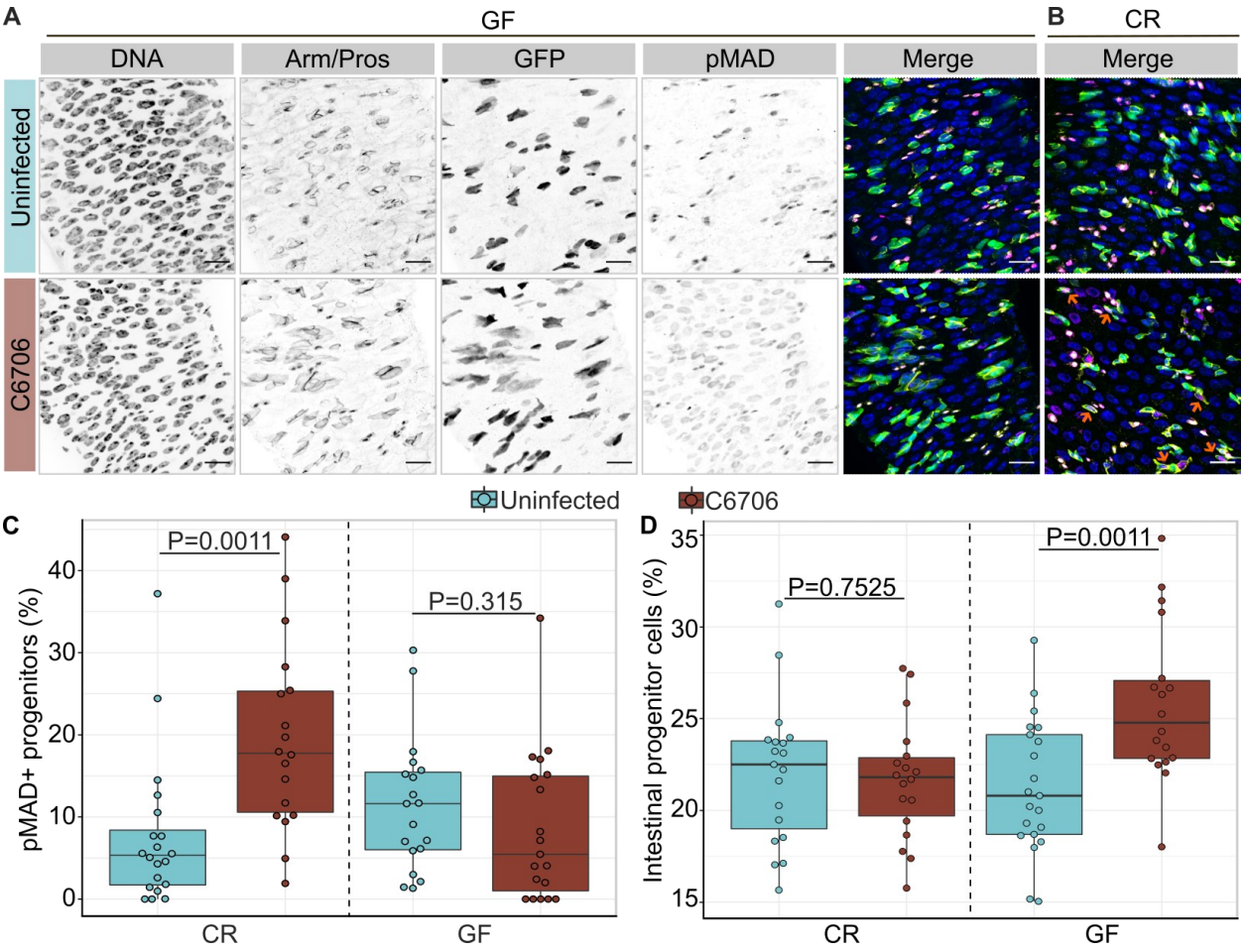

Figure 3.5. Progenitor-specific activation of BMP signaling requires *V. cholerae*-commensal interactions. (A and B) Posterior midguts of **(A)** germ-free (GF) or **(B)** conventionally reared (CR) *esg*^{ts}*/+* adult flies uninfected or infected with C6706 for 24 h. Hoechst labels DNA (blue), Armadillo and Prospero (Arm/Pros) label cell borders and enteroendocrine cells, respectively (yellow), GFP labels progenitors (green), and pMAD labels cells with BMP activation (magenta). Orange arrows indicate pMAD+ GFP+ progenitors. Scale bars = 15 μm. **(C)** Percentage of GFP+ progenitors that are pMAD+ in GF and CR *esg*^{ts}*/+* flies. **(D)** Proportion of GFP+ progenitors in all intestinal epithelial cells in GF and CR *esg*^{ts}*/+* flies. Each dot represents a measurement from a single fly gut. P values are calculated using unpaired Student t-tests.

As the TNFR-like Immune Deficiency (IMD) pathway orchestrates gut responses to commensal bacteria (33,134), and IMD prevents ISC proliferation upon *V. cholerae* infection (31), I then asked if *V. cholerae*-commensal interaction activates BMP via IMD. To probe links between *V. cholerae*, IMD, and BMP, I compared progenitor-specific BMP activation in wild-type and *imd* null mutant (*imd-/-*) flies challenged with C6706. In agreement with Figures 3.2 and 3.5, I again found that infection with *V. cholerae* significantly increased the number of pMAD+ progenitors (small, Arm-enriched, Pros-negative cells) in wildtype host midguts (Figures 3.6A and 3.6C). In contrast, without functional IMD in the midgut, C6706 failed to induce BMP activation in intestinal progenitors (Figures 3.6B and 3.6C).

Next, I wanted to determine the cell type(s) where IMD controls the host response to *V. cholerae* infection. I first knocked down *relish*, which encodes an NF-κB family transcription factor in the IMD pathway, exclusively in progenitors, and measured MAD phosphorylation. Without Relish activity in progenitor cells ($esg^{ts}>rel^{RNAi}$), *V. cholerae* infection still induced BMP activation with a significant increase in numbers of pMAD+ progenitors compared to uninfected counterparts (Figures 3.7A and 3.7C), suggesting that *V. cholerae*-responsive BMP activation does not require IMD-Relish response in progenitors. In contrast, *V. cholerae* infection failed to activate BMP with *relish* depletion from absorptive enterocytes ($MyoIA^{ts}>rel^{RNAi}$) (Figures 3.7B and 3.7D), indicating that enterocyte-specific IMD is essential for BMP activation during *V. cholerae* infection. *V. cholerae*-responsive BMP activation requires IMD activity in enterocytes. As a whole, the data point to a T6SS-dependent activation of progenitor-specific BMP requires pathogen-commensal interactions and host innate immune responses.

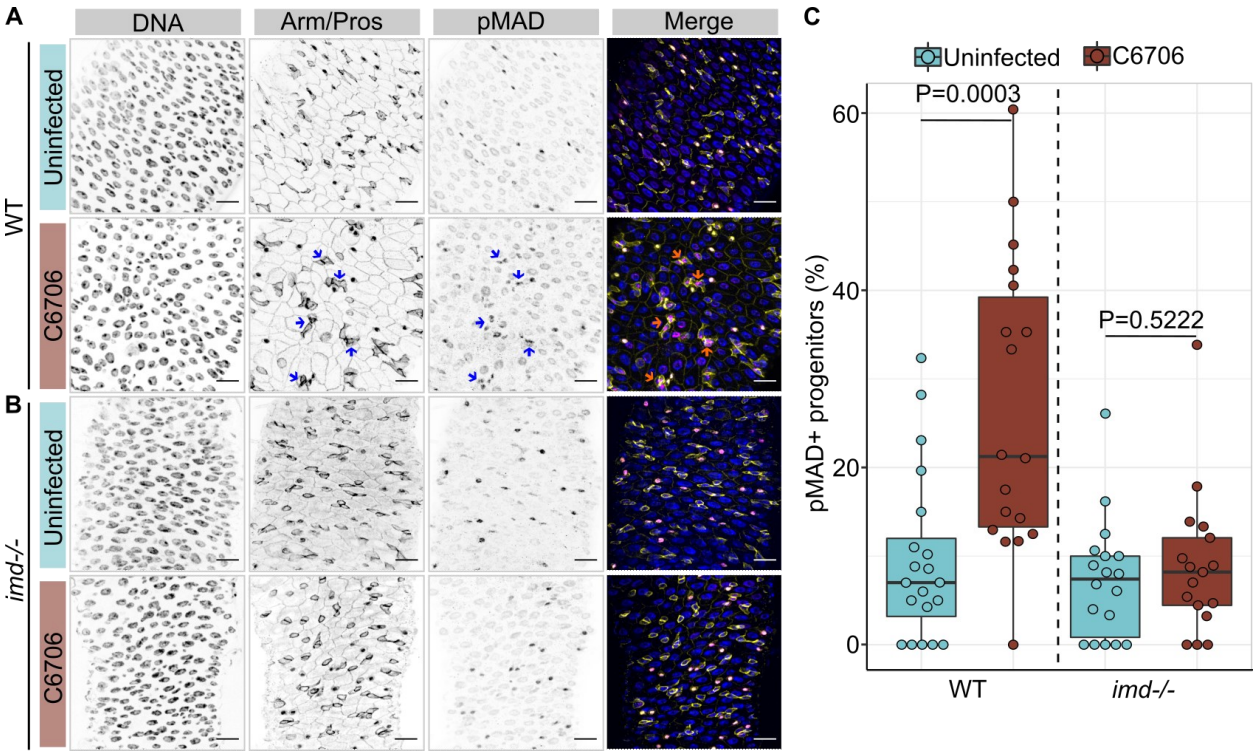

Figure 3.6. *V. cholerae*-responsive activation of BMP requires IMD activity.

(A and B) Posterior midguts of **(A)** wild-type (WT) or **(B)** *imd* null mutant *(imd-/-*) adult flies uninfected or infected with C6706 for 24 h. Hoechst labels DNA (blue), Armadillo and Prospero (Arm/Pros) label cell borders and enteroendocrine cells, respectively (yellow), and pMAD labels cells with BMP activation (magenta). Arrows = pMAD+ progenitor cells. Scale bars = 15 μm. **(C)** Percentage of progenitors that are pMAD+ in WT and *imd-/-* flies. Each dot represents a measurement from a single fly gut. P values are calculated using unpaired Student t-tests.

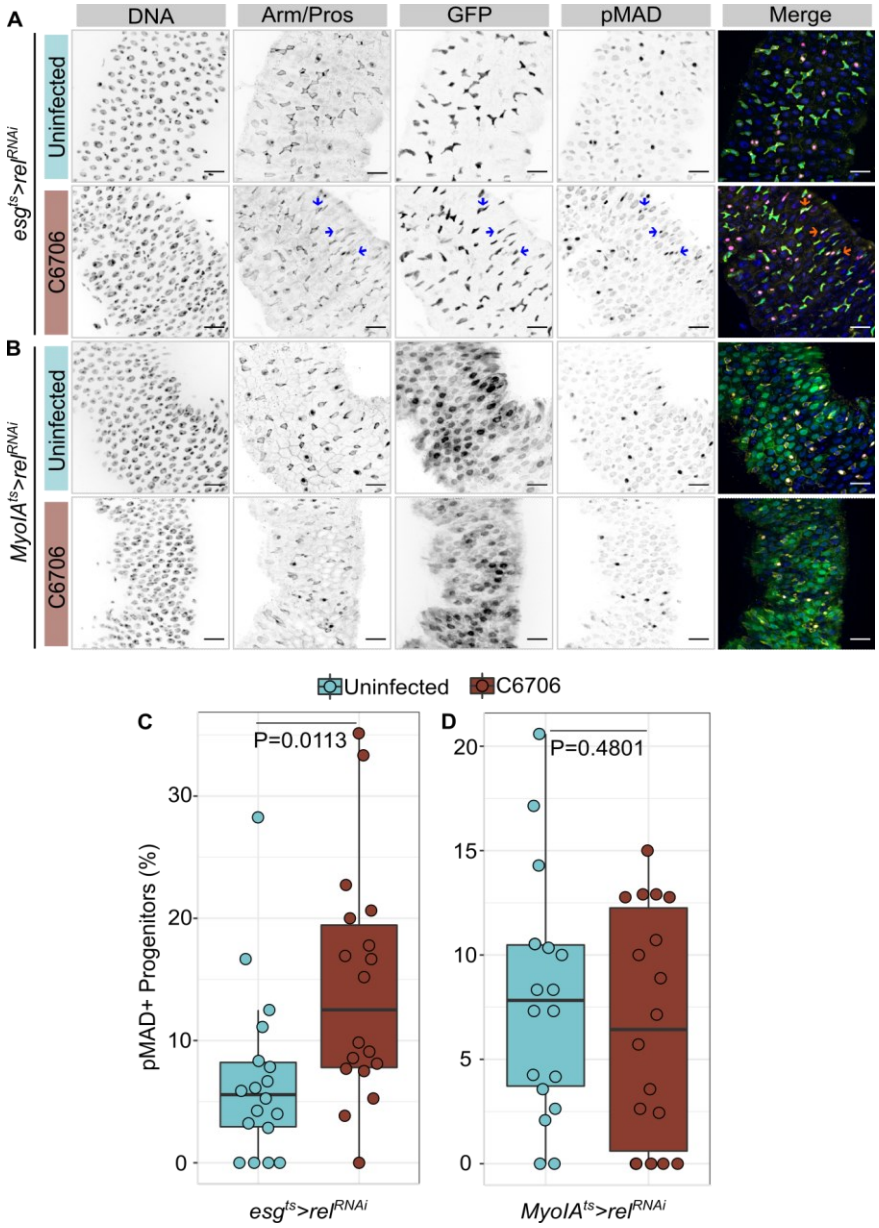

Figure 3.7. Enterocyte-specific IMD is essential for BMP activation during *V. cholerae* infection. (A and B) Posterior midguts of **(A)** *esg*^{ts}*>rel*^{RNAi} or **(B)** *MyoIA*^{ts}*>rel*^{RNAi} adult flies uninfected or infected with C6706 for 24 h. DNA marked by Hoechst (blue), Armadillo and Prospero (Arm/Pros) label cell borders and enteroendocrine cells, respectively (yellow), GFP marks progenitors in *esg*^{ts}*>rel*^{RNAi} flies and enterocytes in *MyoIA*^{ts}*>rel*^{RNAi} flies (green), and pMAD (magenta) to monitor BMP activation. Arrowheads = pMAD+ progenitors. Scale bars = 15 μm. **(C and D)** Percentages of pMAD+ progenitors in **(C)** *esg*^{ts}*>rel*^{RNAi} intestines and **(D)** *MyoIA*^{ts}*>rel*^{RNAi} intestines. Each dot represents a measurement from a single fly gut. P values are calculated using unpaired Student t-tests.

3.3. *V. cholerae*-Dependent Activation of BMP is Essential to Arrest Epithelial Repair in Infected Flies

Thus far, our data are consistent with a link between BMP activation by the T6SS and an arrest of progenitor cell expansion. However, we lack phenotypic data that specifically determine if BMP activation is essential for T6SS-dependent progenitor growth arrest. As T6SS-deficient C6706Δ*vasK* failed to activate BMP or arrest progenitor expansion (Figures 3.2C and 3.4), I first tested if progenitor-specific activation of BMP blocks ISC proliferation in flies challenged with T6SS-deficient *V. cholerae*. Specifically, I compared progenitor cell expansion in control $esg^{ts}/+$ flies and in flies that expressed a constitutively active variant of the type-I BMP receptor *tkv* ($esg^{ts}>tkv^{CA}$) in progenitors. There was a significant expansion of GFP+ progenitor cells in infected $esg^{ts}/+$ guts, confirming activation of the repair response upon damage (Figures 3.8A and 3.8C). In contrast, C6706Δ*vasK* failed to stimulate compensatory progenitor growth in $esg^{ts}>tkv^{CA}$ guts (Figures 3.8B and 3.8C), demonstrating that progenitor-specific BMP is sufficient to arrest epithelial repair in an infected host.

In addition to preventing C6706Δ*vasK*-driven progenitor cell expansion, activation of the BMP pathway had visible effects on the intestinal epithelium of uninfected flies (Figure 3.8B), including a substantial decline in the number of intestinal progenitors (Figure 3.8C). Thus, while interesting, effects of $esg^{ts}>tkv^{CA}$ on host responses to T6SS-deficient C6706Δ*vasK* do not adequately establish a requirement for BMP to arrest progenitor renewal after infection. To directly test if BMP modifies host responses to *V. cholerae*, I specifically ablated BMP signaling in the progenitor compartment by knocking down the transcription factor *shn* ($esg^{ts}>shn^{RNAi}$) and monitored progenitor numbers in flies challenged with wild-type C6706 with a competent T6SS. As anticipated, wild-type *V. cholerae* did not stimulate compensatory progenitor growth in infected $esg^{ts}/+$ flies (Figures 3.8D, 3.8F, and 3.9). However, loss of BMP activity in progenitors effectively ablated *V. cholerae*-mediated inhibition of progenitor growth. Infected $esg^{ts}>shn^{RNAi}$ flies contained a significantly larger number of progenitors and more PH3+ proliferating cells than their uninfected counterparts, similar to what was found in wild-type guts upon challenge with T6SS-deficient *V. cholerae* (Figures 3.8D-F and 3.9). Together, these data demonstrate that BMP in the progenitor compartment is necessary to arrest epithelial repair upon *V. cholerae* infection.

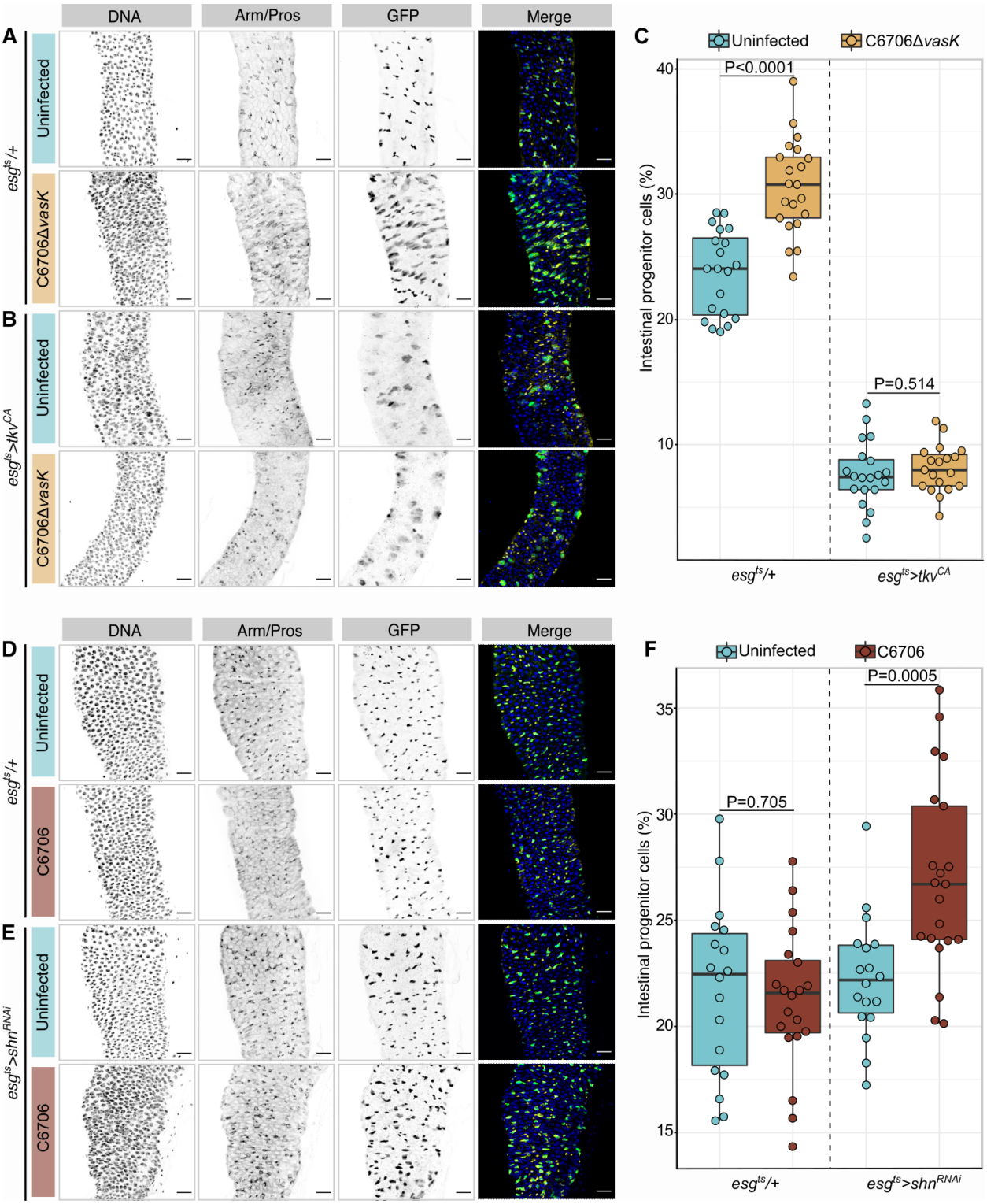

Figure 3.8. BMP regulates epithelial repair after *V. cholerae* infection.

(A and B) Posterior midguts from **(A)** wide-type (*esg*^{ts}*/+*) or **(B)** progenitor-specific BMP activation (*esg*^{ts}*>tkv*^{CA}) adult flies uninfected or infected with C6706Δ*vasK* for 36h. DNA

labeled with Hoechst (blue), GFP marks progenitors (green), Armadillo (Arm) labels cell borders and Prospero (Pros) labels enteroendocrine cells (yellow). Scale bar = 25 μm. **(C)** Proportion of cells that are GFP+ progenitors in *esg^{ts}/+* and *esg^{ts}>tkv^{CA}* flies. Each dot represents a measurement from a single fly gut. P values are calculated using unpaired Student t-tests. **(D and E)** Images of **(D)** wide-type (*esg^{ts}/+*) or **(E)** progenitor-specific BMP inhibition (*esg^{ts}>shn^{RNAi}*) adult flies uninfected or infected with C6706 for 36h. DNA labeled with Hoechst (blue), GFP marks progenitors (green), Armadillo (Arm) labels cell borders and Prospero (Pros) labels enteroendocrine cells (yellow). Scale bar = 25 μm. **(F)** Proportion of cells that are GFP+ progenitors in *esg^{ts}/+* and *esg^{ts}>shn^{RNAi}* flies. Each dot represents a measurement from a single fly gut. P values are calculated using unpaired Student t-tests.

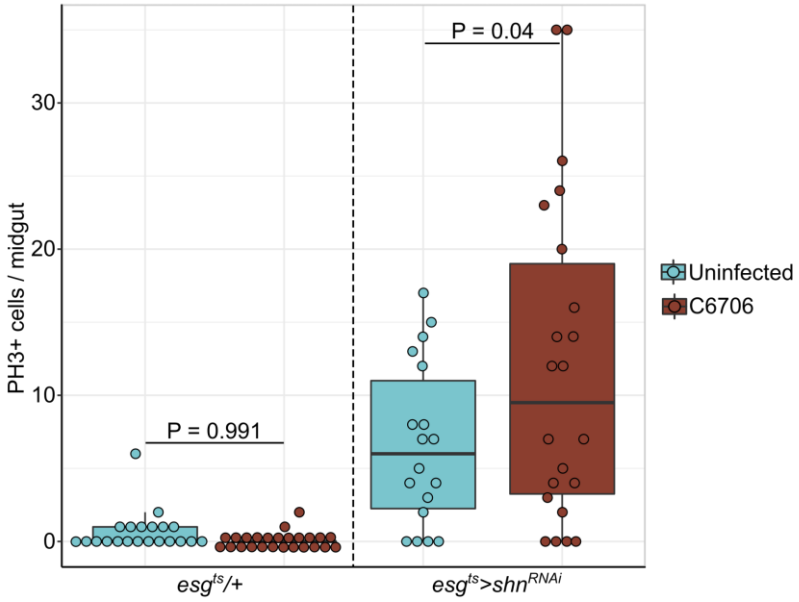

Figure 3.9. BMP regulates cell proliferation upon *V. cholerae* infection. PH3+ cell per midgut in wild-type flies (*esg^{ts}/+*) or progenitor-specific shn knockdown flies (*esg^{ts}>shn^{RNAi}*) upon infection with C6706 for 36h. Each dot represents a measurement from a single fly gut. P values are calculated using unpaired Student t-tests.

3.4 BMP-dependent arrest of proliferation requires a non-autonomous signal from EBs to ISCs

As progenitor cells consist of self-renewing ISCs and transient EBs, I next identified the exact progenitor cell type required for BMP-dependent arrest of epithelial repair. To test if *V. cholerae* activates BMP in a specific progenitor cell type (ISC or EB), I used the EB driver line *Su(H)^{ts}>GFP* that marks EBs with GFP and Dl-expressing ISCs were counterstained by anti-Dl antibody (Figure 1F). I challenged *Su(H)^{ts}/+* flies with C6706 and quantified the number of pMAD+ ISCs (Dl+, GFP-) and pMAD+ EBs (Dl-, GFP+) in the posterior midguts. In both infected and uninfected guts, there were similar and relatively low amounts of ISCs with BMP activity (Figures 3.10A and 3.10B). In contrast, infection with C6706 stimulated a more than threefold increase in the percentages of pMAD+ EBs (Figures 3.10A and 3.10B), indicating that *V. cholerae* infection preferentially activates BMP in EBs. To test the impact of EB-specific BMP activation on epithelial renewal during infection, I knocked down *shn* exclusively in EBs (*Su(H)^{ts}>shn^{RNAi}*) and quantified progenitors after infection. I discovered that, like progenitor-wide knockdown, EB-specific loss of *shn* ablated *V. cholerae*-responsive arrest of progenitor growth (Figure 3.10C). Specifically, the expansion of progenitors was a result of an increased population of ISCs not EBs (Figures 3.10D and 3.10E). Recent studies showed that inactivation of BMP in EBs induces ISC proliferation under homeostatic conditions or during bacterial infections (135). Here, my results reveal that *V. cholerae* infection primarily activates BMP in EBs, which blocks stem cell proliferation and therefore impairs epithelial renewal non-cell autonomously.

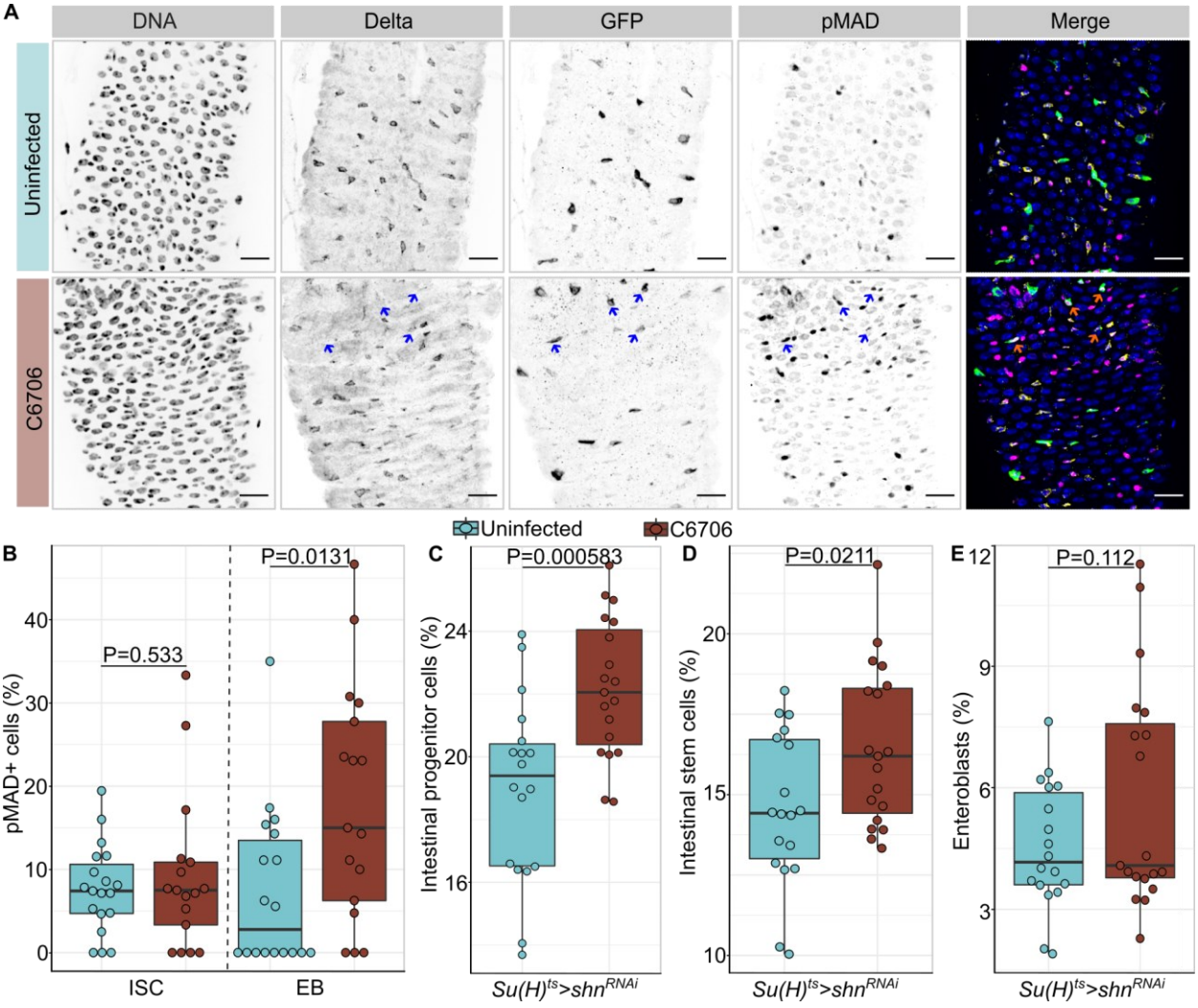

Figure 3.10. *V. cholerae*-responsive BMP activation in EBs arrests intestinal stem cell growth non-cell autonomously. (A) Posterior midguts of uninfected or C6706 infected *Su(H)^{ts}/+* adult flies. DNA marked by Hoechst (blue), Delta (Dl)+ intestinal stem cells (yellow), Su(H)+ EBs marked by GFP (green), and pMAD (magenta) to monitor BMP activation. Arrowheads = pMAD+ EBs (Dl- and GFP+). Scale bars = 15 μm. **(B)** Proportion of intestinal stem cells or EBs that are pMAD+ in *Su(H)^{ts}/+* intestines. **(C-E)** Proportions of all cells that are **(C)** progenitors, **(D)** intestinal stem cells, or **(E)** EBs in the intestines with EB-specific BMP inactivation (*Su(H)^{ts}>shn^{RNAi}*). Each dot represents a measurement from a single fly gut. P values are calculated using Student t-tests.

3.5 The T6SS suppresses cell proliferation and induces TGF-β/BMP activation in a vertebrate intestine.

To expand our study, I then asked if the impact of the *V. cholerae* T6SS on intestinal epithelial renewal applies to vertebrate hosts. Zebrafish *Danio rerio* are ideal vertebrate models to study *V. cholerae* pathogenesis (70,118,119). Fish intestines are naturally colonized by *Vibrio* species and develop cholera-like symptoms upon *V. cholerae* infection (118–122). Importantly, like the mammalian intestine, the zebrafish intestinal epithelium contains a complex community of secretory and absorptive lineages that interact with immune-regulatory myeloid and lymphoid cells (123–126).

As enteric infection normally causes damage to the gut, I first tested if *V. cholerae* T6SS impacts epithelial damage. In the absence of infection, adult fish intestines contained a limited number of TUNEL+ apoptotic cells (Figure 3.11A). Infection with *V. cholerae* disrupted epithelial integrity and significantly increased the amount of dying cells (Figure 3.11A). Moreover, wild-type C6706-infected guts contained approximately twice as many TUNEL+ cells as in the T6SS-deficient C6706Δ*vasK*-infected counterparts, indicating that *V. cholerae* T6SS promoted epithelial damage (Figures 3.11A and 3.11B).

Next, to test whether *V. cholerae* T6SS impacts epithelial repair in fish, I challenged zebrafish larvae and adults with either wildtype C6706 or C6706Δ*vasK* and measured cell proliferation. In fish larvae, uninfected intestines contained moderate amounts of EdU+ proliferating cells (Figures 3.11C and 3.11D). Infection with C6706Δ*vasK* promoted epithelial repair indicated by a significantly higher proliferation rate compared to uninfected guts (Figures 3.11C and 3.11D). In contrast, there was no significant difference in the numbers of EdU+ cells between C6706-infected and uninfected guts. In parallel to these findings in larvae, I also discovered that the *V. cholerae* T6SS disrupts IEC regeneration in adult zebrafish intestines. Both C6706 and C6706Δ*vasK* damaged the intestinal epithelium, characterized by disorganized IECs and lumenal shedding of damaged tissue (Figure 3.11E). Damage in C6706Δ*vasK*-infected guts stimulated repair, as the numbers of PCNA+ proliferating cells nearly doubled compared to uninfected counterparts (Figures 3.11E and 3.11F). However, I did not detect significant changes in cell proliferation rates after C6706

infection (Figures 3.11E and 3.11F). These data demonstrate that, like in a fly host, *V. cholerae* arrests epithelial proliferation in zebrafish intestines in a T6SS-dependent manner.

Furthermore, I found that the T6SS induced TGF-β/BMP activity, as zebrafish larvae infected with wildtype *V. cholerae* contained significantly larger numbers of cells with an active, phosphorylated form of SMAD3 (pSMAD3) compared to the uninfected and T6SS-deficient *V. cholerae* infected counterparts (Figures 3.12A and 3.12B). Although further studies are needed to determine whether TGF-β/BMP activity is necessary for T6SS-responsive arrest of cell proliferation, these findings raise the possibility that *V. cholerae* blocks intestinal epithelial repair upon damage through similar mechanisms in invertebrates and vertebrates.

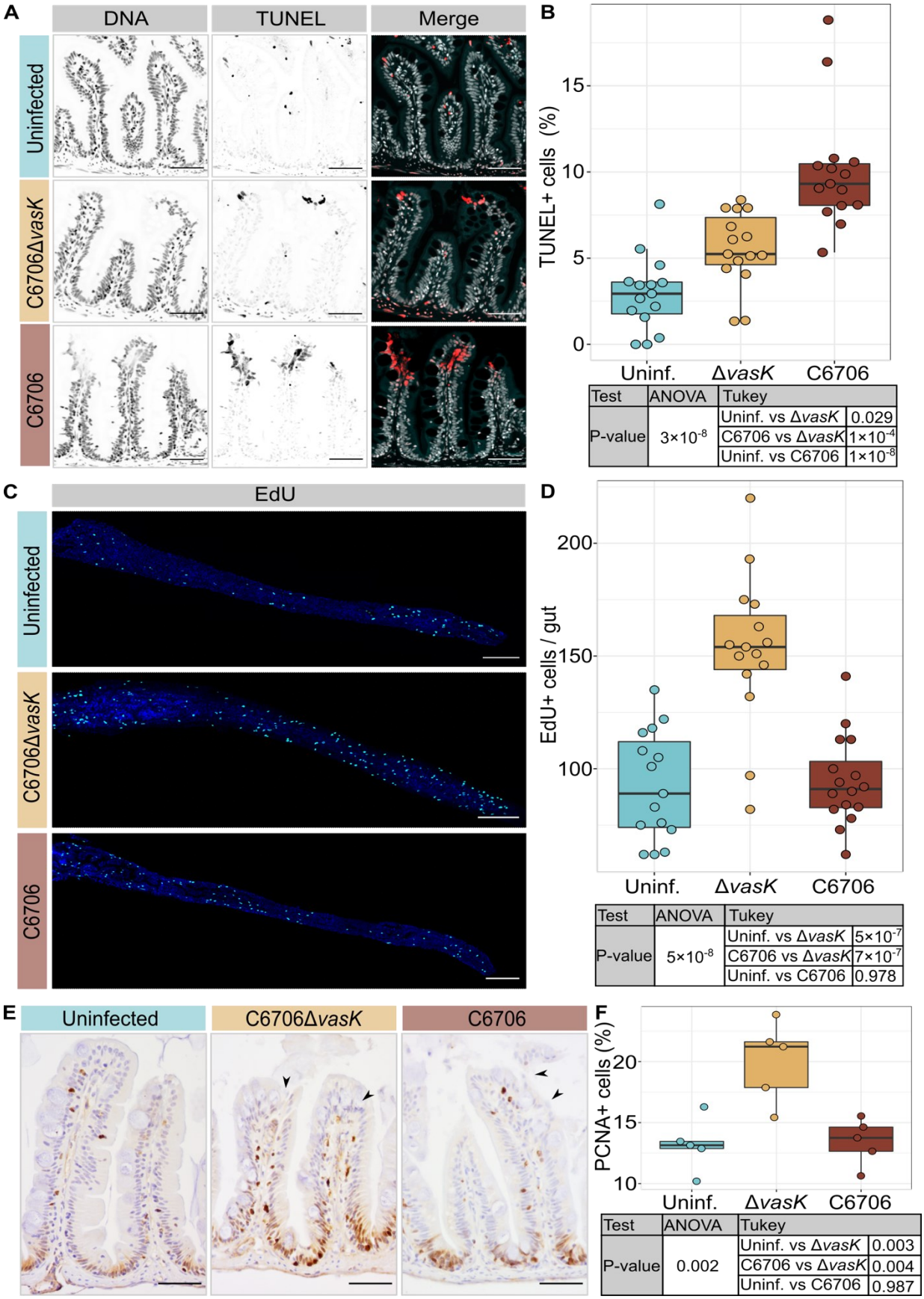
A
DNA
TUNEL
Merge
Uninfected
C6706ΔvasK
C6706
B
TUNEL+ cells (%)
0
5
10
15
Uninf.
ΔvasK
C6706
Test | ANOVA | Tukey
P-value | 3×10-8 | Uninf. vs ΔvasK | 0.029
C6706 vs ΔvasK | 1×10-4
Uninf. vs C6706 | 1×10-8
C
EdU
Uninfected
C6706ΔvasK
C6706
D
EdU+ cells / gut
100
150
200
Uninf.
ΔvasK
C6706
Test | ANOVA | Tukey
P-value | 5×10-8 | Uninf. vs ΔvasK | 5×10-7
C6706 vs ΔvasK | 7×10-7
Uninf. vs C6706 | 0.978
E
Uninfected
C6706ΔvasK
C6706
F
PCNA+ cells (%)
10
15
20
Uninf.
ΔvasK
C6706
Test | ANOVA | Tukey
P-value | 0.002 | Uninf. vs ΔvasK | 0.003
C6706 vs ΔvasK | 0.004
Uninf. vs C6706 | 0.987

Figure 3.11. *V. cholerae* T6SS promotes damage and limits cell proliferation in the zebrafish intestine.

(A) Adult TL zebrafish intestine uninfected or infected with *V. cholerae.* Hoechst marks DNA in blue and TUNEL+ cells in red. Scale bars = 50 μm. **(B)** Quantification of TUNEL+ intestinal epithelial cells. N=5 for each condition. For each fish, three images were taken from different positions in the posterior intestine. Each dot represents the quantification from a single image. P values are calculated using the significance tests indicated in the tables. **(C)** Intestines of uninfected or *V. cholerae*-infected TL zebrafish larvae with DNA stained by Hoechst in blue and EdU+ cells in cyan. Scale bars = 200 μm. **(D)** Quantification of EdU+ cells per gut. Each dot represents a measurement from a single fish intestine. P values are calculated using the significance tests indicated in the tables. **(E)** Immunohistochemical images of sagittal posterior intestinal sections from adult TL zebrafish stained for PCNA. Arrowheads indicate epithelial damages marked by disorganized nuclei and shedding of epithelial cells. Scale bars = 50 μm. **(F)** Percentage of intestinal epithelial cells that are PCNA+ in adult fish posterior intestine. Each dot represents a measurement from a single fish gut.

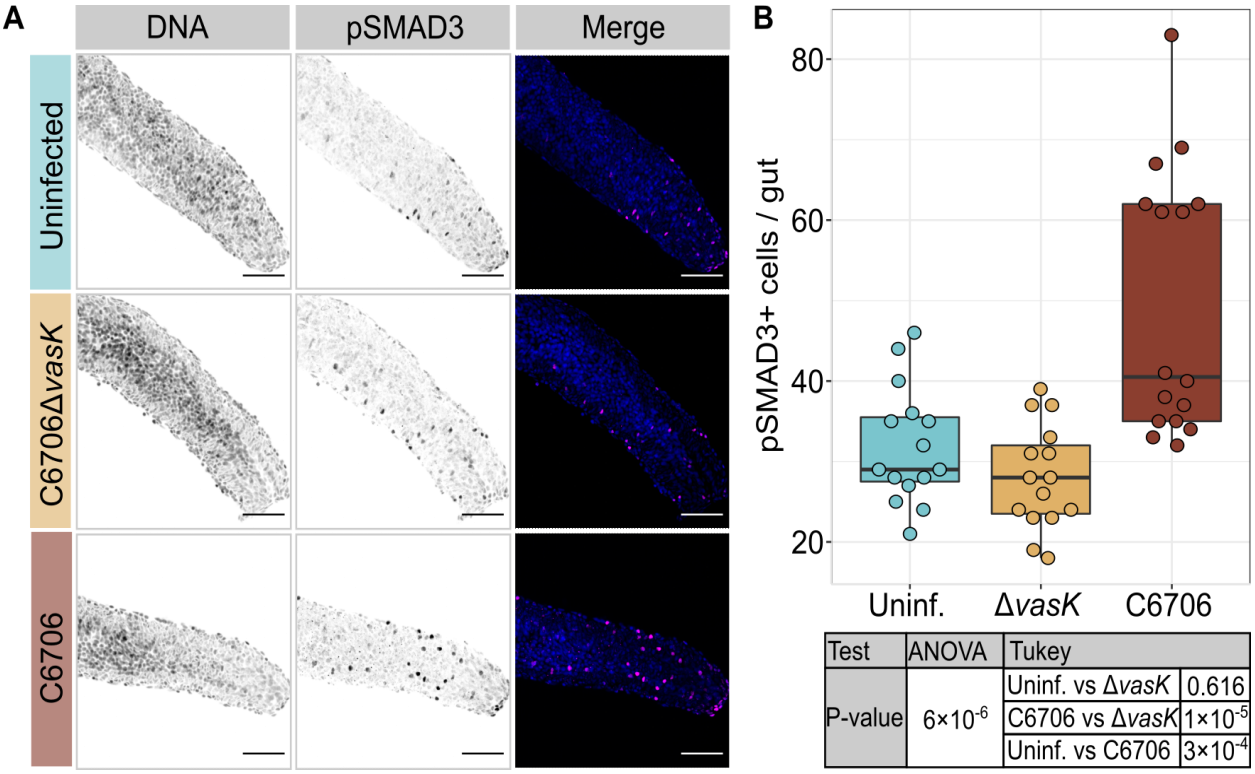

Figure 3.12. *V. cholerae* T6SS induces TGF-β/BMP activation in the zebrafish intestine. **(A)** Posterior intestines from TL zebrafish larvae with DNA marked by Hoechst in blue and pSMAD3 in magenta. Scale bars = 100 μm. **(B)** Quantification of pSMAD3+ cells per gut with each dot representing a single gut. P values are calculated using the significance tests indicated in the table.

Chapter 4

Discussion

This chapter contains content from the following source:

- **Xu, X.** and Foley, E. *Vibrio cholerae* Arrests Intestinal Epithelial Proliferation through T6SS-dependent Activation of the Bone Morphogenetic Protein Pathway. *Cell Reports* (Under Revision). *Biorxiv*.

  doi: https://doi.org/10.1101/2023.06.29.547108

4.1 Summary

Epithelial damage during enteric infections normally accelerates cell proliferation and tissue repair via stress responses such as the epidermal growth factor receptor (EGFR) and Janus kinase-signal transducer and activator of transcription (JAK-STAT) pathways (14,34,36,37). However, oral infection of *Drosophila* with *V. cholerae* arrests intestinal progenitor cell proliferation in a T6SS-dependent manner (30). It is unknown how *V. cholerae* blocks host tissue repair. We consider this an important question, as failure in renewing damaged cells disrupts intestinal barrier integrity and exposes the host to microbial invasions, which increases the risk of systemic infection and potentiates the development of chronic inflammatory illness (34,43).

Within the scope of my thesis, I explored molecular mechanisms of how *V. cholerae* T6SS impacts intestinal epithelial repair upon infections (Figure 4.1). Using the *Drosophila* model, I found that T6SS-commensal interactions induce BMP response specifically in intestinal progenitor cells. Activation of BMP signaling requires IMD/Relish activity in enterocytes. *V. cholerae*-responsive BMP activation is necessary to block epithelial repair upon infection, which is primarily in EBs of the progenitor compartment and arrests ISC proliferation non-cell-autonomously. Furthermore, *V. cholerae* T6SS blocks intestinal proliferation and activates BMP signaling in the vertebrate zebrafish model. Together, this study reveals how pathogen-commensal interactions engage evolutionarily conserved immune and growth regulators to impact intestinal epithelial renewal upon infection and also raises several interesting aspects to be further elucidated.

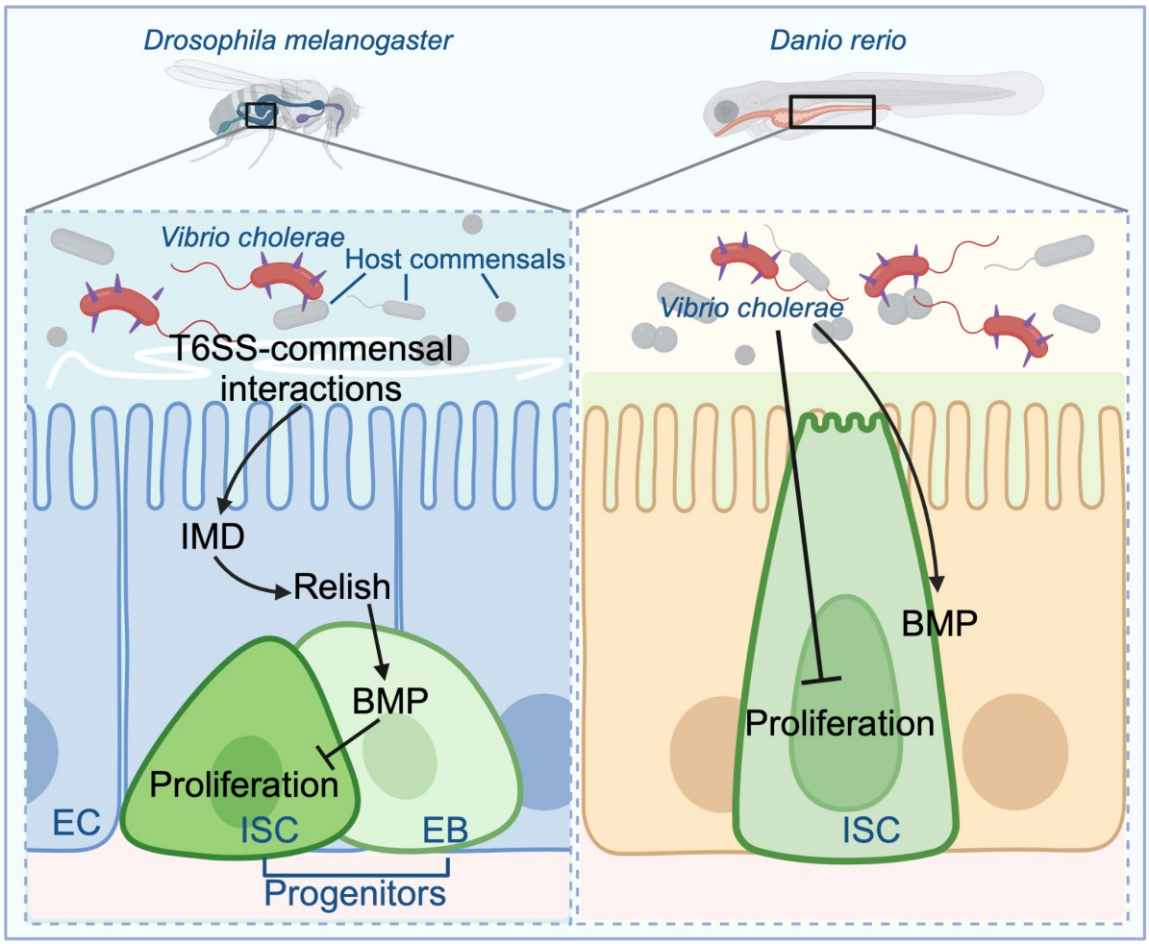

Figure 4.1. Summary model.

In *Drosophila*, interactions between *V. cholerae* T6SS and gut commensals induce BMP responses in enteroblasts (EBs) through IMD/Relish activity in enterocytes (ECs). EB-specific BMP blocks proliferation of intestinal progenitor cells (ISCs) and therefore arrests epithelial repair upon infection. In zebrafish *Danio rerio*, *V. cholerae* infection limits ISC proliferation and induces BMP response in a T6SS-dependent manner.

4.2 How does IMD activate intestinal BMP during *V. cholerae* infections?

Normally, IMD serves a protective role and is essential for surviving infections by bacterial pathogens like *Pseudomonas entomophila* (136–138). In contrast, *V. cholerae*-dependent activation of IMD in the fly gut arrests ISC proliferation and severely shortens the host lifespan (29,31,109). The precise mechanism by which *V. cholerae* signals through the IMD pathway to disrupt gut epithelial barrier remains to be clarified. I found that *V. cholerae*-commensal interactions activate BMP in progenitors in an IMD-dependent manner (Figures 3.6 and 3.7), suggesting a putative IMD-BMP axis in regulating tissue repair upon infection.

4.2.1 Which commensal species are responsible for initiating an IMD-BMP response?

IMD is typically activated by recognition of a bacterial cell wall component, diaminopimelic acid-type peptidoglycan (DAP-PGN) (139–144), although alternate mechanisms also exist in the gut (145). During *V. cholerae* infections, T6SS-dependent killing of gut commensals generates significant amounts of microbial components. Our cultures of *Drosophila* are dominated by gut resident *Acetobacter* and *Lactobacillus*, both containing DAP-PGNs (26,28). Gram-negative *Acetobacter sp.* is sensitive to *V. cholerae* T6SS (109). In addition, T6SS-mediated killing of *A. pasteurianus* accelerates host death and contributes to *V. cholerae* pathogenesis (109). Therefore, it is possible that microbial components generated by T6SS-*Acetobacter sp.* interactions initiate IMD response in the gut. However, interactions between *V. cholerae* T6SS and *A. pasteurianus* alone are not sufficient to block intestinal epithelial repair (30), indicating that other commensal species are involved in *V. cholerae*-responsive activation of an IMD-BMP axis to impact tissue renewal (Figure 4.2).

Current evidence suggests that Gram-positive bacteria like *Lactobacillus sp.* are naturally immune to T6SS attacks, likely due to an increased thickness of PGN cell wall, which prevents T6SS to penetrate and deliver toxic effectors at effective concentrations (146). However, a recent study showed that *Acinetobacter baumannii* employs its T6SS to kill different Gram-positive bacteria (147). Specifically, *A. baumannii* modifies its microenvironment to enhance the PGN-degrading activity of the T6SS effector Tse4. Tse4 represents a broad family of T6SS effectors that share a similar modular architecture in which the endopeptidase, lytic transglycosylase, and PGN-binding domains are lined in different arrangements (147). A genome-wide analysis showed that *V. cholerae* T6SS

auxiliary gene cluster 4 encodes a predicted effector Tse4 (148). Therefore, we cannot completely exclude the possibility that *V. cholerae* T6SS may attack certain Gram-positive commensals in the fly gut, generating cell wall components that initiate IMD responses. Together, these findings suggest that activation of an IMD-BMP axis during *V. cholerae* infection may require complex interactions between the T6SS and a consortium of intestinal symbionts. Given the ease of reconstituting gut microbiota in *Drosophila*, further studies in gnotobiotic flies would be helpful to identify the commensal species involved in *V. cholerae*-responsive activation of an IMD-BMP regulatory axis that blocks repair of damaged tissue (Figure 4.2).

4.2.2 How does IMD-NF-κB activity induce BMP response in the gut?

All cell types within the intestinal epithelium encode IMD pathway components (149). In response to infectious microbes, the IMD pathway signals the NF-κB-like transcription factor, Relish, to upregulate expression of antimicrobial peptides and regulators of the IMD pathway in epithelial cells (149). It seems that IMD is primarily activated in ECs during *V. cholerae* infection, as these large absorptive cells are the most abundant epithelial cell type and make direct contact with the intestinal lumen where they can detect DAP-PGN. Besides its bactericidal function, EC-specific IMD activity plays an important role in maintaining tissue homeostasis. Deregulation of IMD specifically in ECs triggers progenitor hyperproliferation and dysplasia (150). Upon bacterial infection, activation of the IMD-Relish pathway in ECs triggers shedding of damaged ECs in a cell-autonomous manner (150). In this thesis, I found that EC-specific IMD-Relish activity is essential to activate BMP signaling in intestinal progenitors during *V. cholerae* infections (Figures 3.6 and 3.7). It is unknown how IMD response in ECs regulates BMP response in progenitors (Figure 4.2). Recent studies established a link between NF-κB and BMP signaling. NF-κB can directly regulate BMP responses cell-autonomously. Activation of NF-κB by lipopolysaccharides inhibits phosphorylation and nuclear translocation of BMP pathway transcription factors SMAD1/5/8 and therefore suppresses BMP signaling activity (151). NF-κB also controls the production of BMP ligands to indirectly regulate BMP response. Mechanistically, NF-κB binds to bmp2 promoter and transactivates gene expression, inducing autocrine production of BMP2 ligands (152,153). In the *Drosophila* intestine, ECs are a major source of BMP ligands

(53,154). EC-derived BMP serves as a niche signal that regulates ISC self-renewal (154). Collectively, these findings lead to my hypothesis that NF-κB-mediated transactivation of genes encoding BMP ligands in ECs results in secretion of BMP ligands from ECs, which activate BMP signaling in neighboring progenitor cells in a paracrine manner. Given the importance of BMP and TNFR-like signalings in regulating tissue homeostasis, in-depth studies would be required to thoroughly examine this hypothesis and elucidate crosstalk between these two pathways.

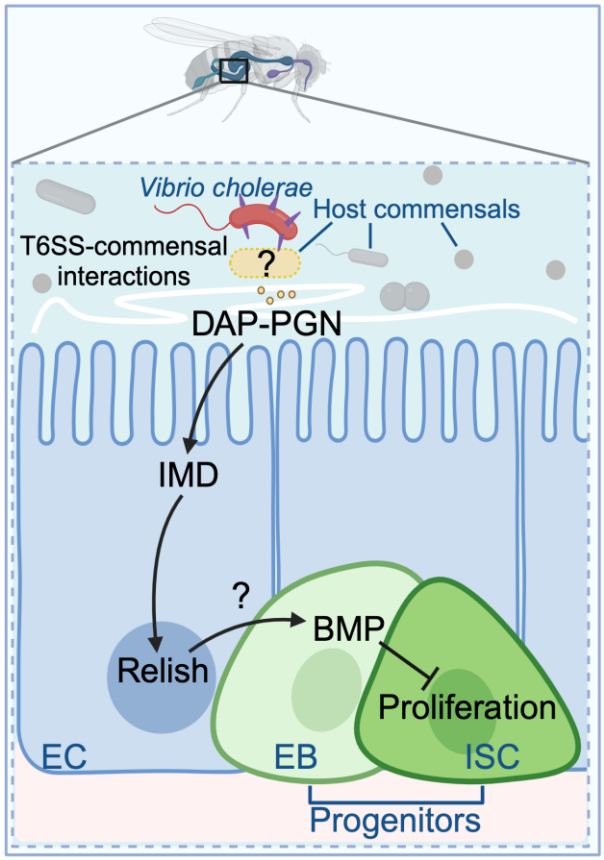

Figure 4.2. *V. cholerae*-responsive BMP activation requires IMD-Relish activity. T6SS-mediated killing of commensals generates bacterial cell wall components that activate the IMD pathway. IMD-Relish activity in ECs is essential to induce progenitor-specific BMP activation upon *V. cholerae* infections. The identity of commensal species targeted by *V. cholerae* T6SS and mechanisms of Relish-dependent BMP activation are unknown.

4.3 How does BMP regulate ISC proliferation upon *V. cholerae* infections?

BMP signaling is essential to the development and homeostasis of the intestine (46). Within the scope of this thesis, I uncovered a non-cell autonomous role of BMP signaling in regulating gut epithelial renewal during infection (Figure 3.9). Specifically, *V. cholerae*-responsive BMP activation in EBs blocks proliferation of neighboring ISCs. Currently, it is unclear how EB-specific BMP activity regulates ISC proliferation. Several studies have demonstrated a non-autonomous role of BMP signaling in the fly gut. Loss of BMP signaling in ECs fuels ISC proliferation (154,155). EB-specific BMP inactivation stimulates ISC hyperproliferation upon challenges with the fly pathogen *Ecc15* or in the absence of infection (58). In the mammalian intestine, while early studies suggested that BMP signaling autonomously restricts ISC proliferation by directly inhibiting the Wnt/β-catenin activity (42,156), later work showed that BMP signaling in stromal cells indirectly suppresses ISC proliferation (157). Specifically, loss of SMAD4 in T cells led to epithelial cancers in mice intestines, whereas epithelial-specific-deletion of the Smad4 gene did not (157). Together, these findings demonstrate a critical role of non-autonomous BMP in regulating intestinal epithelial homeostasis. Typically, epithelial damage during enteric infections activates stress responses like JAK-STAT and EGFR signalings in ISCs, accelerating cell proliferation (14,34,36,37). A recent work revealed a functional link between BMP and stress responses in regulating intestinal epithelial renewal in *Drosophila*. Specifically, loss of BMP signaling induces an ectopic activation of JAK-STAT and EGFR signalings in fly midguts, which fuel stem cell division and eventually disrupt intestinal homeostasis (155). Our transcriptional data showed that wildtype *V. cholerae* with competent T6SSs does not induce JAK-STAT and EGFR activities in progenitor cells, whereas T6SS-deficient *V. cholerae* successfully initiates both responses upon infection (30). Thus, I speculate that BMP activity in EBs blocks epithelial proliferation by antagonizing JAK-STAT or EGFR responses in neighboring ISCs upon *V. cholerae* infections. Further investigations are required to elucidate the mechanisms by which BMP non-autonomously regulates stem cell growth during enteric infections.

4.4 How does BMP regulate epithelial homeostasis during enteric infections in vertebrates?

Regulated BMP response is essential to protect vertebrates from intestinal diseases. For instance, upregulation of BMP activity in vertebrate intestines alleviates intestinal inflammation, prevents intestinal fibrosis, and limits colitis formation (65–67). In contrast, loss of BMP activity causes hyperplasia, elevated inflammation, and tumor growth in the intestine (42,60,61). Despite the importance of BMP signaling in intestinal epithelial homeostasis, we know very little about BMP involvement in vertebrate responses to enteric infections. Within the scope of this thesis, I found that T6SS-responsive activation of BMP blocks ISC proliferation, leading to an arrest of epithelial repair during *V. cholerae* infection. Notably, these findings are not restricted to flies (Figures 3.2, 3.5, and 3.8). Using a vertebrate zebrafish model, I found that *V. cholerae* T6SS induces TGF-β/BMP activity in the intestine (Figure 3.11). Moreover, *V. cholerae* infection suppresses cell proliferation in a T6SS-dependent manner despite widespread damage to the fish intestinal epithelium (Figure 3.10). It remains to be seen that *V. cholerae* infection induces BMP activation in which cell type(s) and whether the cell type-specific BMP response is necessary to block epithelial repair in the fish gut (Figure 4.3). Besides, there are several interesting aspects to be further elucidated.

4.4.1 Are host immune responses involved in regulating intestinal epithelial renewal during *V. cholerae* infection?

Unlike fly guts which mainly rely on germline-encoded innate defenses, zebrafish intestines possess both innate immune responses and lymphocyte-based adaptive defenses that impact host responses to symbiotic and pathogenic microbes (124,126,158–163). A recent study from our group characterized how *V. cholerae* infection modifies immune responses in adult zebrafish intestines (126). We observed that *V. cholerae* infection enhances expression of proinflammatory genes and genes associated with antigen presentation in intestinal epithelial cells (126). Exposure to *V. cholerae* also recruits and activates gut-associated T cells (126). We also found that *V. cholerae* suppresses expression of interferon signaling genes in both epithelial cells and macrophages, indicating a unifying

mechanism of cell response to *V. cholerae* (126). Together, these data provide insights into host-pathogen interactions and expand the utility of zebrafish as a vertebrate model in resolving gut immune responses to *V. cholerae* infection. Recent studies revealed an immune-modulatory role of BMP in the vertebrate intestine (157,164,165). In both human and mouse colons, epithelial-specific BMP activity limits expression of pro-inflammatory genes including a number of chemokines and cytokines and suppresses infiltration of macrophages and neutrophils (164,165). Loss of BMP pathway transcription factor SMAD4 in epithelial cells promotes inflammation-driven carcinogenesis in mouse colon (164,166). Based on these findings and advantages of the zebrafish model, future studies could be conducted in fish to determine whether epithelial BMP signaling synergizes with innate and adaptive defenses to regulate intestinal epithelial barrier during *V. cholerae* infections (Figure 4.3).

4.4.2 How does T6SS-commensal interaction impact intestinal epithelial repair?

Bacterial symbionts form a barrier that shields the intestinal epithelium, constantly interacting with microbial invaders (167). Using its T6SS, *V. cholerae* outcompetes gut commensals to colonize the intestinal epithelium, replicate, and persist for a prolonged period. Studies have demonstrated that the T6SS contributes to *V. cholerae* pathogenesis besides its role in promoting colonization. For instance, T6SS-commensal interactions enhance host innate immune responses and the development of diarrhea disease symptoms in both flies and vertebrates (30,108,109,168). Moreover, studies from our lab showed that T6SS-symbiont interactions impair intestinal progenitor cell proliferation in fly guts and therefore block tissue repair (Figure 3.5)(30). Using our vertebrate zebrafish model, I uncovered a T6SS-dependent arrest of cell proliferation in both larvae and adults (Figure 3.10). It is still unclear whether gut commensals are required for T6SS-responsive arrest of epithelial repair in the vertebrate intestine. Further analysis of cell proliferation and BMP activity in germ-free zebrafish would help to test if pathogen-commensal interactions engage evolutionarily conserved regulators and mechanisms to impact host responses (Figure 4.3).

4.4.3 Does prior exposure to T6SS affect host responses on re-exposure to *V. cholerae*?

Infection with *V. cholerae* elicits long-term protections against subsequent diseases (169,170). Although the mechanism remains unclear, it has been suggested that memory B cells in the gut-associated lymphoid tissue play a key role in protective immunity (170,171). Following an acute infection, cholera patients develop significant B cell responses against *V. cholerae* antigens including lipopolysaccharide, cholera toxin B subunit, and toxin-coregulated pilus major subunit A, and these memory B cells remain detectable in the circulation for more than one year (170). Besides the protective immunity, variation in composition of gut microbiome confers variable resistance to *V. cholerae* infection (172). As T6SS-mediated killing of commensals significantly changes the composition of gut microbiome and contributes to *V. cholerae* pathogenesis and disease development, it is worth studying if pathogen-symbiont interactions impact secondary responses to *V. cholerae* re-exposure (168).

T6SS contact-dependent attacking of the gut microbiome results in a decreased proportion of susceptible commensal species and an expansion of T6SS-resistant microbes in the gut (108). *V. cholerae* T6SS also affects composition of gut commensals through a number of mechanisms independent of direct killing. For example, *V. cholerae* uses its T6SS to increase host gut contractility for expelling resident bacteria in the zebrafish intestine (107). Additionally, T6SS-commensal interactions enhance the severity of diarrhea symptoms, which disrupts native gut microbial communities. Specifically, T6SS-mediated killing of symbionts induces mucin production, a marker for diarrhea, and upregulates virulence genes encoding cholera toxin that contribute to the diarrheal disease (108,168). During profuse watery diarrhea, the diversity of the gut microbiome drops dramatically, and the gut is dominated by Streptococci, Enterococci, and Proteobacteria (172,173).

Although Gram-positive bacteria like Streptococci and Enterococci are considered to be resistant to T6SS due to an increased thickness of bacterial cell wall (146), a recent study uncovered T6SS effectors degrading cell wall of Gram-positive species (147). More than 50% of ß- and γ-proteobacteria are T6SS-positive and produce immunity proteins against toxic T6SS effectors (89,174). However, challenged by diverse competitors in various

environments, different bacterial species and even different strains of the same species secrete different combinations of effectors to promote intraspecific and interspecific competition (175,176). Therefore, it remains to be further examined how re-exposure to *V. cholerae* impacts composition of the gut microbiota. Given the essential role of T6SS-commensal interactions in *V. cholerae* pathogenesis, I hypothesize that changes in composition of the gut microbiome upon an acute *V. cholerae* infection may impact host susceptibility to the re-exposure of the same pathogen, potentially affecting epithelial regeneration upon infections and disease severity. Future studies about impacts of T6SS-microbe interactions on host secondary responses would provide us insights into the mechanism of protective immunity in cholera patients developed after an acute infection and the role of gut commensals during enteric infections (Figure 4.3).

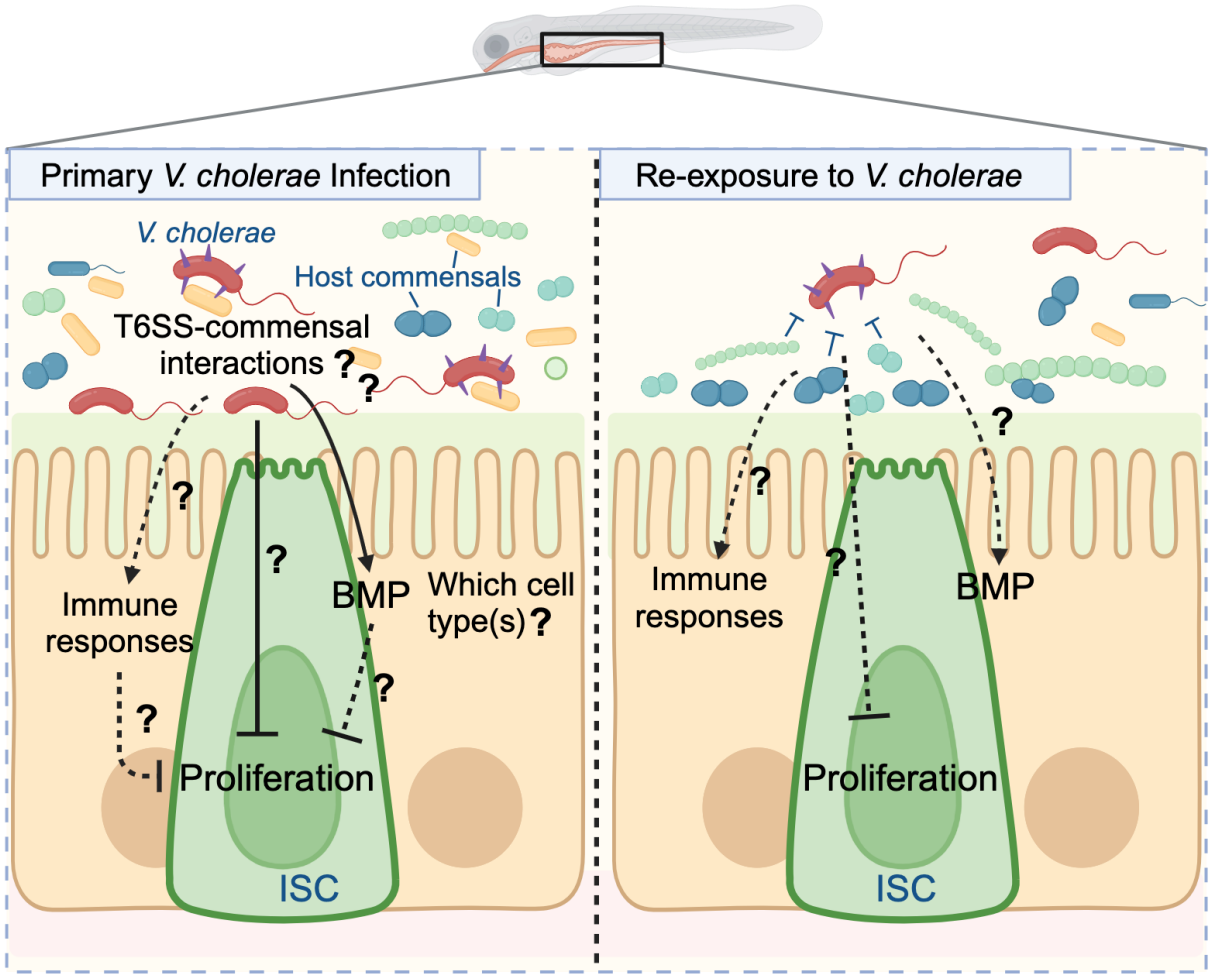

Figure 4.3. *V. cholerae* blocks intestinal epithelial repair in the zebrafish intestine.

V. cholerae infection blocks intestinal stem cell proliferation and activates BMP response in a T6SS-dependent manner, but the underlying mechanisms remain unclear. It is also unknown if pathogen-commensal interactions, host immune responses or BMP activity are required for T6SS-dependent arrest of epithelial repair. It also remains in question if prior exposure to T6SS affects host responses to re-exposure to *V. cholerae*.

4.5 Concluding remarks

During enteric infections, the replacement of damaged tissue by intestinal progenitor cells is vital to maintain the epithelial barrier and protect the host from systemic infection. *V. cholerae* causes widespread destruction to the intestinal epithelium and blocks tissue repair by limiting progenitor proliferation. The underlying molecular mechanisms of *V. cholerae*-responsive arrest of epithelial renewal remain unclear. Within the scope of my thesis, I found that T6SS-commensal interactions modify host immune and growth regulatory pathways to disrupt intestinal epithelial repair during *V. cholerae* infection. Using the *Drosophila* model, I uncovered effects of the BMP pathway and innate immune response, the TNFR-like IMD pathway, on progenitor proliferation upon *V. cholerae* infection. In addition, I found that *V. cholerae* blocks epithelial repair and activates BMP response in the vertebrate zebrafish model. Given the importance of BMP and TNFR-like signalings in regulating intestinal homeostasis, I consider this work relevant to understand how pathogen-commensal interactions orchestrate host responses to a global health threat.

Bibliography

1. Hakim RS, Baldwin K, Smagghe G. Regulation of midgut growth, development, and metamorphosis. Annu Rev Entomol. 2010;55:593–608.

2. Buchon N, Osman D, David FPA, Yu Fang H, Boquete JP, Deplancke B, et al. Morphological and Molecular Characterization of Adult Midgut Compartmentalization in Drosophila. Cell Rep. 2013 May 30;3(5):1725–38.

3. Dubreuil RR, Grushko T, Baumann O. Differential effects of a labial mutation on the development, structure, and function of stomach acid-secreting cells in Drosophila melanogaster larvae and adults. Cell Tissue Res. 2001 Oct 1;306(1):167–78.

4. Takashima S, Mkrtchyan M, Younossi-Hartenstein A, Merriam JR, Hartenstein V. The behaviour of Drosophila adult hindgut stem cells is controlled by Wnt and Hh signalling. Nature. 2008 Jul;454(7204):651–5.

5. Micchelli CA, Perrimon N. Evidence that stem cells reside in the adult Drosophila midgut epithelium. Nature. 2006 Jan;439(7075):475–9.

6. Ohlstein B, Spradling A. The adult Drosophila posterior midgut is maintained by pluripotent stem cells. Nature. 2006 Jan;439(7075):470–4.

7. Ohlstein B, Spradling A. Multipotent Drosophila Intestinal Stem Cells Specify Daughter Cell Fates by Differential Notch Signaling. Science. 2007 Feb 16;315(5814):988–92.

8. Casali A, Batlle E. Intestinal Stem Cells in Mammals and Drosophila. Cell Stem Cell. 2009 Feb 6;4(2):124–7.

9. Jiang H, Edgar BA. Intestinal stem cells in the adult Drosophila midgut. Exp Cell Res. 2011 Nov 15;317(19):2780–8.

10. Jiang H, Edgar BA. Intestinal stem cell function in Drosophila and mice. Curr Opin Genet Dev. 2012 Aug 1;22(4):354–60.

11. Takashima S, Adams KL, Ortiz PA, Ying CT, Moridzadeh R, Younossi-Hartenstein A, et al. Development of the Drosophila entero-endocrine lineage and its specification by the Notch signaling pathway. Dev Biol. 2011 May 15;353(2):10.1016/j.ydbio.2011.01.039.

12. Kuraishi T, Binggeli O, Opota O, Buchon N, Lemaitre B. Genetic evidence for a protective role of the peritrophic matrix against intestinal bacterial infection in Drosophila melanogaster. Proc Natl Acad Sci. 2011 Sep 20;108(38):15966–71.

13. Lin G, Xu N, Xi R. Paracrine Wingless signalling controls self-renewal of Drosophila intestinal stem cells. Nature. 2008 Oct;455(7216):1119–23.

14. Jiang H, Grenley MO, Bravo MJ, Blumhagen RZ, Edgar BA. EGFR/Ras/MAPK Signaling Mediates Adult Midgut Epithelial Homeostasis and Regeneration in Drosophila. Cell Stem Cell. 2011 Jan 7;8(1):84–95.

15. Biteau B, Jasper H. EGF signaling regulates the proliferation of intestinal stem cells in Drosophila. Development. 2011 Mar 15;138(6):1045–55.

16. Guo Z, Driver I, Ohlstein B. Injury-induced BMP signaling negatively regulates Drosophila midgut homeostasis. J Cell Biol. 2013 Jun 10;201(6):945–61.

17. Kleino A, Silverman N. The Drosophila IMD pathway in the activation of the humoral immune response. Dev Comp Immunol. 2014 Jan;42(1):10.1016/j.dci.2013.05.014.

18. Myllymäki H, Valanne S, Rämet M. The Drosophila imd signaling pathway. J Immunol Baltim Md 1950. 2014 Apr 15;192(8):3455–62.

19. Choe KM, Lee H, Anderson KV. Drosophila peptidoglycan recognition protein LC (PGRP-LC) acts as a signal-transducing innate immune receptor. Proc Natl Acad Sci U S A. 2005 Jan 25;102(4):1122–6.

20. Kleino A, Ramia NF, Bozkurt G, Shen Y, Nailwal H, Huang J, et al. Peptidoglycan-Sensing Receptors Trigger the Formation of Functional Amyloids of the Adaptor Protein Imd to Initiate Drosophila NF-κB Signaling. Immunity. 2017 Oct 17;47(4):635-647.e6.

21. Paquette N, Broemer M, Aggarwal K, Chen L, Husson M, Ertürk-Hasdemir D, et al. Caspase-Mediated Cleavage, IAP Binding, and Ubiquitination: Linking Three Mechanisms Crucial for Drosophila NF-κB Signaling. Mol Cell. 2010 Jan 29;37(2):172–82.

22. Dushay MS, Asling B, Hultmark D. Origins of immunity: Relish, a compound Rel-like gene in the antibacterial defense of Drosophila. Proc Natl Acad Sci U S A. 1996 Sep 17;93(19):10343–7.

23. Silverman N, Zhou R, Stöven S, Pandey N, Hultmark D, Maniatis T. A Drosophila IκB kinase complex required for Relish cleavage and antibacterial immunity. Genes Dev. 2000 Oct 1;14(19):2461–71.

24. Stöven S, Ando I, Kadalayil L, Engström Y, Hultmark D. Activation of the Drosophila NF-κB factor Relish by rapid endoproteolytic cleavage. EMBO Rep. 2000 Oct 16;1(4):347–52.

25. Boutros M, Agaisse H, Perrimon N. Sequential Activation of Signaling Pathways during Innate Immune Responses in Drosophila. Dev Cell. 2002 Nov 1;3(5):711–22.

26. Shin M, Ferguson M, Willms RJ, Jones LO, Petkau K, Foley E. Immune regulation of intestinal-stem-cell function in Drosophila. Stem Cell Rep. 2022 Apr 12;17(4):741–55.

27. Liu X, Nagy P, Bonfini A, Houtz P, Bing XL, Yang X, et al. Microbes affect gut epithelial cell composition through immune-dependent regulation of intestinal stem cell differentiation. Cell Rep. 2022 Mar 29;38(13):110572.

28. Petkau K, Ferguson M, Guntermann S, Foley E. Constitutive Immune Activity Promotes Tumorigenesis in Drosophila Intestinal Progenitor Cells. Cell Rep. 2017 Aug 22;20(8):1784–93.

29. Berkey CD, Blow N, Watnick PI. Genetic analysis of Drosophila melanogaster susceptibility to intestinal Vibrio cholerae infection. Cell Microbiol. 2009 Mar;11(3):461–74.

30. Fast D, Petkau K, Ferguson M, Shin M, Galenza A, Kostiuk B, et al. Vibrio cholerae-Symbiont Interactions Inhibit Intestinal Repair in Drosophila. Cell Rep. 2020 Jan 28;30(4):1088-1100.e5.

31. Wang Z, Hang S, Purdy AE, Watnick PI. Mutations in the IMD Pathway and Mustard Counter Vibrio cholerae Suppression of Intestinal Stem Cell Division in Drosophila. mBio. 2013 Jun 18;4(3):e00337-13.

32. Amcheslavsky A, Jiang J, Ip YT. Tissue Damage-Induced Intestinal Stem Cell Division in Drosophila. Cell Stem Cell. 2009 Jan 9;4(1):49–61.

33. Buchon N, Broderick NA, Poidevin M, Pradervand S, Lemaitre B. Drosophila Intestinal Response to Bacterial Infection: Activation of Host Defense and Stem Cell Proliferation. Cell Host Microbe. 2009 Feb 19;5(2):200–11.

34. Buchon N, Broderick NA, Chakrabarti S, Lemaitre B. Invasive and indigenous microbiota impact intestinal stem cell activity through multiple pathways in Drosophila. Genes Dev. 2009 Oct 1;23(19):2333–44.

35. Kim M, Ashida H, Ogawa M, Yoshikawa Y, Mimuro H, Sasakawa C. Bacterial Interactions with the Host Epithelium. Cell Host Microbe. 2010 Jul 22;8(1):20–35.

36. Buchon N, Broderick NA, Kuraishi T, Lemaitre B. Drosophila EGFR pathway coordinates stem cell proliferation and gut remodeling following infection. BMC Biol. 2010 Dec 22;8:152.

37. Jiang H, Patel PH, Kohlmaier A, Grenley MO, McEwen DG, Edgar BA. Cytokine/Jak/Stat Signaling Mediates Regeneration and Homeostasis in the Drosophila Midgut. Cell. 2009 Jun 26;137(7):1343–55.

38. Sato T, Vries RG, Snippert HJ, van de Wetering M, Barker N, Stange DE, et al. Single Lgr5 stem cells build crypt-villus structures in vitro without a mesenchymal niche. Nature. 2009 May;459(7244):262–5.

39. Sato T, van Es JH, Snippert HJ, Stange DE, Vries RG, van den Born M, et al. Paneth cells constitute the niche for Lgr5 stem cells in intestinal crypts. Nature. 2011 Jan;469(7330):415–8.

40. Herrera SC, Bach EA. JAK/STAT signaling in stem cells and regeneration: from Drosophila to vertebrates. Dev Camb Engl. 2019 Jan 15;146(2):dev167643.

41. Hong AW, Meng Z, Guan KL. The Hippo pathway in intestinal regeneration and disease. Nat Rev Gastroenterol Hepatol. 2016 Jun;13(6):324–37.

42. He XC, Zhang J, Tong WG, Tawfik O, Ross J, Scoville DH, et al. BMP signaling inhibits intestinal stem cell self-renewal through suppression of Wnt–β-catenin signaling. Nat Genet. 2004 Oct;36(10):1117–21.

43. Rera M, Clark RI, Walker DW. Intestinal barrier dysfunction links metabolic and inflammatory markers of aging to death in Drosophila. Proc Natl Acad Sci U S A. 2012 Dec 26;109(52):21528–33.

44. Su YH, Chen YC, Ting HC, Fan TP, Lin CY, Wang KT, et al. BMP controls dorsoventral and neural patterning in indirect-developing hemichordates providing insight into a possible origin of chordates. Proc Natl Acad Sci. 2019 Jun 25;116(26):12925–32.

45. Sconocchia T, Sconocchia G. Regulation of the Immune System in Health and Disease by Members of the Bone Morphogenetic Protein Family. Front Immunol. 2021 Dec 2;12:802346.

46. Shroyer NF, Wong MH. BMP Signaling in the Intestine: Cross-Talk Is Key. Gastroenterology. 2007 Sep 1;133(3):1035–8.

47. Upadhyay A, Moss-Taylor L, Kim MJ, Ghosh AC, O'Connor MB. TGF-β Family Signaling in Drosophila. Cold Spring Harb Perspect Biol. 2017 Sep 1;9(9):a022152.

48. Savin T, Kurpios NA, Shyer AE, Florescu P, Liang H, Mahadevan L, et al. On the growth and form of the gut. Nature. 2011 Aug;476(7358):57–62.

49. Nerurkar NL, Mahadevan L, Tabin CJ. BMP signaling controls buckling forces to modulate looping morphogenesis of the gut. Proc Natl Acad Sci. 2017 Feb 28;114(9):2277–82.

50. Karlsson L, Lindahl P, Heath JK, Betsholtz C. Abnormal gastrointestinal development in PDGF-A and PDGFR-α deficient mice implicates a novel mesenchymal structure with putative instructive properties in villus morphogenesis. Development. 2000 Aug 15;127(16):3457–66.

51. Walton KD, Kolterud Å, Czerwinski MJ, Bell MJ, Prakash A, Kushwaha J, et al. Hedgehog-responsive mesenchymal clusters direct patterning and emergence of intestinal villi. Proc Natl Acad Sci. 2012 Sep 25;109(39):15817–22.

52. Walton KD, Whidden M, Kolterud Å, K. Shoffner S, Czerwinski MJ, Kushwaha J, et al. Villification in the mouse: Bmp signals control intestinal villus patterning. Dev Camb Engl. 2016 Feb 1;143(3):427–36.

53. Li H, Qi Y, Jasper H. Dpp Signaling Determines Regional Stem Cell Identity in the Regenerating Adult Drosophila Gastrointestinal Tract. Cell Rep. 2013 Jul 11;4(1):10–8.

54. Auclair BA, Benoit YD, Rivard N, Mishina Y, Perreault N. Bone Morphogenetic Protein Signaling Is Essential for Terminal Differentiation of the Intestinal Secretory Cell Lineage. Gastroenterology. 2007 Sep 1;133(3):887–96.

55. Berková L, Fazilaty H, Yang Q, Kubovčiak J, Stastna M, Hrckulak D, et al. Terminal differentiation of villus tip enterocytes is governed by distinct Tgfβ superfamily members. EMBO Rep. 2023 Jul 26;e56454.

56. Barker N, van Es JH, Kuipers J, Kujala P, van den Born M, Cozijnsen M, et al. Identification of stem cells in small intestine and colon by marker gene Lgr5. Nature. 2007 Oct 25;449(7165):1003–7.

57. Qi Z, Li Y, Zhao B, Xu C, Liu Y, Li H, et al. BMP restricts stemness of intestinal Lgr5+ stem cells by directly suppressing their signature genes. Nat Commun. 2017 Jan 6;8(1):13824.

58. Zhou J, Florescu S, Boettcher AL, Luo L, Dutta D, Kerr G, et al. Dpp/Gbb signaling is required for normal intestinal regeneration during infection. Dev Biol. 2015 Mar 15;399(2):189–203.

59. Howe JR, Roth S, Ringold JC, Summers RW, Järvinen HJ, Sistonen P, et al. Mutations in the SMAD4/DPC4 Gene in Juvenile Polyposis. Science. 1998 May 15;280(5366):1086–8.

60. Howe J, Sayed M, Ahmed A, Ringold J, Larsen-Haidle J, Merg A, et al. The prevalence of MADH4 and BMPR1A mutations in juvenile polyposis and absence of BMPR2, BMPR1B, and ACVR1 mutations. J Med Genet. 2004 Jul;41(7):484–91.

61. Haramis APG, Begthel H, van den Born M, van Es J, Jonkheer S, Offerhaus GJA, et al. De Novo Crypt Formation and Juvenile Polyposis on BMP Inhibition in Mouse Intestine. Science. 2004 Mar 12;303(5664):1684–6.

62. Andriopoulos B, Corradini E, Xia Y, Faasse SA, Chen S, Grgurevic L, et al. BMP-6 is a key endogenous regulator of hepcidin expression and iron metabolism. Nat Genet. 2009 Apr;41(4):482–7.

63. Meynard D, Kautz L, Darnaud V, Canonne-Hergaux F, Coppin H, Roth MP. Lack of the bone morphogenetic protein BMP6 induces massive iron overload. Nat Genet. 2009 Apr;41(4):478–81.

64. Stein J, Hartmann F, Dignass AU. Diagnosis and management of iron deficiency anemia in patients with IBD. Nat Rev Gastroenterol Hepatol. 2010 Nov;7(11):599–610.

65. Wang L, Trebicka E, Fu Y, Ellenbogen S, Hong CC, Babitt JL, et al. The Bone Morphogenetic Protein–Hepcidin Axis as a Therapeutic Target in Inflammatory Bowel Disease. Inflamm Bowel Dis. 2012 Jan 1;18(1):112–9.

66. Maric I, Poljak L, Zoricic S, Bobinac D, Bosukonda D, Sampath KT, et al. Bone morphogenetic protein-7 reduces the severity of colon tissue damage and accelerates the healing of inflammatory bowel disease in rats. J Cell Physiol. 2003;196(2):258–64.

67. Koppens MAJ, Davis H, Valbuena GN, Mulholland EJ, Nasreddin N, Colombe M, et al. Bone Morphogenetic Protein Pathway Antagonism by Grem1 Regulates Epithelial Cell Fate in Intestinal Regeneration. Gastroenterology. 2021 Jul 1;161(1):239-254.e9.

68. Utada AS, Bennett RR, Fong JCN, Gibiansky ML, Yildiz FH, Golestanian R, et al. Vibrio cholerae use pili and flagella synergistically to effect motility switching and conditional surface attachment. Nat Commun. 2014 Sep 19;5(1):4913.

69. Conner JG, Teschler JK, Jones CJ, Yildiz FH. Staying alive: Vibrio cholerae's cycle of environmental survival, transmission, and dissemination. Microbiol Spectr. 2016 Apr;4(2):10.1128/microbiolspec.VMBF-0015–2015.

70. Mitchell KC, Withey JH. Danio rerio as a Native Host Model for Understanding Pathophysiology of Vibrio cholerae. Methods Mol Biol Clifton NJ. 2018;1839:97–102.

71. Fotedar R. Vector potential of houseflies (Musca domestica) in the transmission of Vibrio cholerae in India. Acta Trop. 2001 Jan 15;78(1):31–4.

72. Echeverria P, Harrison BA, Tirapat C, McFarland A. Flies as a source of enteric pathogens in a rural village in Thailand. Appl Environ Microbiol. 1983 Jul;46(1):32–6.

73. Laviad-Shitrit S, Sela R, Thorat L, Sharaby Y, Izhaki I, Nath BB, et al. Identification of chironomid species as natural reservoirs of toxigenic Vibrio cholerae strains with pandemic potential. PLoS Negl Trop Dis. 2020 Dec 23;14(12):e0008959.

74. Almagro-Moreno S, Taylor RK. Cholera: Environmental Reservoirs and Impact on Disease Transmission. Microbiol Spectr. 2013 Dec;1(2):OH-0003-2012.

75. Ali M, Nelson AR, Lopez AL, Sack DA. Updated Global Burden of Cholera in Endemic Countries. PLoS Negl Trop Dis. 2015 Jun 4;9(6):e0003832.

76. Mintz E. Taking aim at cholera. The Lancet. 2018 May 12;391(10133):1868–70.

77. Alexakis LC. Cholera -"Rice water stools. Pan Afr Med J. 2017 Mar 14;26:147.

78. Sharifi-Mood B, Metanat M. Diagnosis, Clinical Management, Prevention, and Control of Cholera; A Review Study. Int J Infect. 2014;1(1).

79. Yemen: Cholera Response Weekly Epidemiological Bulletin: W26 2018 (Jun 25 - Jul 01) [EN/AR] - Yemen | ReliefWeb [Internet]. 2018 [cited 2023 Oct 10]. Available from: https://reliefweb.int/report/yemen/yemen-cholera-response-weekly-epidemiological-bulletin-w26-2018-jun-25-jul-01-enar

80. Das B, Verma J, Kumar P, Ghosh A, Ramamurthy T. Antibiotic resistance in Vibrio cholerae: Understanding the ecology of resistance genes and mechanisms. Vaccine. 2020 Feb 29;38:A83–92.

81. Bart KJ, Huq Z, Khan M, Mosley WH, Nuruzzaman Md, Golam Kibriya AKM. Seroepidemiologic Studies during a Simultaneous Epidemic of Infection with El Tor Ogawa and Classical Inaba Vibrio cholerae. J Infect Dis. 1970 May 1;121(Supplement):S17–24.

82. Sack RB, Siddique AK, Longini IM Jr, Nizam A, Yunus Md, Islam MS, et al. A 4-Year Study of the Epidemiology of Vibrio cholerae in Four Rural Areas of Bangladesh. J Infect Dis. 2003 Jan 1;187(1):96–101.

83. Khan M, Shahidullah M. Cholera due to the E1 Tor biotype equals the classical biotype in severity and attack rates. J Trop Med Hyg. 1980 Feb;83(1):35–9.

84. Murley YM, Behari J, Griffin R, Calderwood SB. Classical and El Tor Biotypes of Vibrio cholerae Differ in Timing of Transcription of tcpPHduring Growth in Inducing Conditions. Infect Immun. 2000 May;68(5):3010–4.

85. Kovacikova G, Skorupski K. Differential Activation of the tcpPH Promoter by AphB Determines Biotype Specificity of Virulence Gene Expression in Vibrio cholerae. J Bacteriol. 2000 Jun;182(11):3228–38.

86. Benitez JA, Silva AJ. Vibrio cholerae hemagglutinin(HA)/protease: an extracellular metalloprotease with multiple pathogenic activities. Toxicon Off J Int Soc Toxinology. 2016 Jun 1;115:55–62.

87. Cordero CL, Sozhamannan S, Satchell KJF. RTX Toxin Actin Cross-Linking Activity in Clinical and Environmental Isolates of Vibrio cholerae. J Clin Microbiol. 2007 Jul;45(7):2289–92.

88. Vaitkevicius K, Lindmark B, Ou G, Song T, Toma C, Iwanaga M, et al. A Vibrio cholerae protease needed for killing of Caenorhabditis elegans has a role in protection from natural predator grazing. Proc Natl Acad Sci U S A. 2006 Jun 13;103(24):9280–5.

89. Boyer F, Fichant G, Berthod J, Vandenbrouck Y, Attree I. Dissecting the bacterial type VI secretion system by a genome wide in silico analysis: what can be learned from available microbial genomic resources? BMC Genomics. 2009 Mar 12;10:104.

90. Leiman PG, Basler M, Ramagopal UA, Bonanno JB, Sauder JM, Pukatzki S, et al. Type VI secretion apparatus and phage tail-associated protein complexes share a common evolutionary origin. Proc Natl Acad Sci. 2009 Mar 17;106(11):4154–9.

91. Brunet YR, Zoued A, Boyer F, Douzi B, Cascales E. The Type VI Secretion TssEFGK-VgrG Phage-Like Baseplate Is Recruited to the TssJLM Membrane Complex via Multiple Contacts and Serves As Assembly Platform for Tail Tube/Sheath Polymerization. PLOS Genet. 2015 Oct 13;11(10):e1005545.

92. MacIntyre DL, Miyata ST, Kitaoka M, Pukatzki S. The Vibrio cholerae type VI secretion system displays antimicrobial properties. Proc Natl Acad Sci. 2010 Nov 9;107(45):19520–4.

93. Shneider MM, Buth SA, Ho BT, Basler M, Mekalanos JJ, Leiman PG. PAAR-repeat proteins sharpen and diversify the type VI secretion system spike. Nature. 2013 Aug;500(7462):350–3.

94. Zoued A, Durand E, Bebeacua C, Brunet YR, Douzi B, Cambillau C, et al. TssK Is a Trimeric Cytoplasmic Protein Interacting with Components of Both Phage-like and Membrane Anchoring Complexes of the Type VI Secretion System. J Biol Chem. 2013 Sep 20;288(38):27031–41.

95. Vettiger A, Winter J, Lin L, Basler M. The type VI secretion system sheath assembles at the end distal from the membrane anchor. Nat Commun. 2017 Jul 13;8(1):16088.

96. Basler M, Mekalanos JJ. Type 6 secretion dynamics within and between bacterial cells. Science. 2012 Aug 17;337(6096):815.

97. Basler M, Pilhofer M, Henderson GP, Jensen GJ, Mekalanos JJ. Type VI secretion requires a dynamic contractile phage tail-like structure. Nature. 2012 Mar;483(7388):182–6.

98. Unterweger D, Kostiuk B, Pukatzki S. Adaptor Proteins of Type VI Secretion System Effectors. Trends Microbiol. 2017 Jan 1;25(1):8–10.

99. Miyata ST, Unterweger D, Rudko SP, Pukatzki S. Dual Expression Profile of Type VI Secretion System Immunity Genes Protects Pandemic Vibrio cholerae. PLOS Pathog. 2013 Dec 5;9(12):e1003752.

100. Dong TG, Ho BT, Yoder-Himes DR, Mekalanos JJ. Identification of T6SS-dependent effector and immunity proteins by Tn-seq in Vibrio cholerae. Proc Natl Acad Sci U S A. 2013 Feb 12;110(7):2623–8.

101. Altindis E, Dong T, Catalano C, Mekalanos J. Secretome Analysis of Vibrio cholerae Type VI Secretion System Reveals a New Effector-Immunity Pair. mBio. 2015 Mar 10;6(2):e00075-15.

102. Brooks TM, Unterweger D, Bachmann V, Kostiuk B, Pukatzki S. Lytic Activity of the Vibrio cholerae Type VI Secretion Toxin VgrG-3 Is Inhibited by the Antitoxin TsaB. J Biol Chem. 2013 Mar 15;288(11):7618–25.

103. Pukatzki S, Ma AT, Revel AT, Sturtevant D, Mekalanos JJ. Type VI secretion system translocates a phage tail spike-like protein into target cells where it cross-links actin. Proc Natl Acad Sci. 2007 Sep 25;104(39):15508–13.

104. Pukatzki S, Ma AT, Sturtevant D, Krastins B, Sarracino D, Nelson WC, et al. Identification of a conserved bacterial protein secretion system in Vibrio cholerae using the Dictyostelium host model system. Proc Natl Acad Sci. 2006 Jan 31;103(5):1528–33.

105. Miyata ST, Kitaoka M, Brooks TM, McAuley SB, Pukatzki S. Vibrio cholerae Requires the Type VI Secretion System Virulence Factor VasX To Kill Dictyostelium discoideum ▿. Infect Immun. 2011 Jul;79(7):2941–9.

106. Ma AT, Mekalanos JJ. In vivo actin cross-linking induced by Vibrio cholerae type VI secretion system is associated with intestinal inflammation. Proc Natl Acad Sci. 2010 Mar 2;107(9):4365–70.

107. Logan SL, Thomas J, Yan J, Baker RP, Shields DS, Xavier JB, et al. The Vibrio cholerae type VI secretion system can modulate host intestinal mechanics to displace gut bacterial symbionts. Proc Natl Acad Sci. 2018 Apr 17;115(16):E3779–87.

108. Zhao W, Caro F, Robins W, Mekalanos JJ. Antagonism toward the intestinal microbiota and its effect on Vibrio cholerae virulence. Science. 2018 Jan 12;359(6372):210–3.

109. Fast D, Kostiuk B, Foley E, Pukatzki S. Commensal pathogen competition impacts host viability. Proc Natl Acad Sci. 2018 Jul 3;115(27):7099–104.

110. Chiang SL, Mekalanos JJ. Use of signature-tagged transposon mutagenesis to identify Vibrio cholerae genes critical for colonization. Mol Microbiol. 1998;27(4):797–805.

111. Herrington DA, Hall RH, Losonsky G, Mekalanos JJ, Taylor RK, Levine MM. Toxin, toxin-coregulated pili, and the toxR regulon are essential for Vibrio cholerae pathogenesis in humans. J Exp Med. 1988 Oct 1;168(4):1487–92.

112. Klose KE. The suckling mouse model of cholera. Trends Microbiol. 2000 Apr;8(4):189–91.

113. Matson JS. Infant Mouse Model of Vibrio cholerae Infection and Colonization. In: Sikora AE, editor. Vibrio Cholerae: Methods and Protocols. New York, NY: Springer; 2018. p. 147–52. (Methods in Molecular Biology).

114. Tanaka M, Nakayama J. Development of the gut microbiota in infancy and its impact on health in later life. Allergol Int. 2017 Oct 1;66(4):515–22.

115. Olivier V, Salzman NH, Satchell KJF. Prolonged Colonization of Mice by Vibrio cholerae El Tor O1 Depends on Accessory Toxins. Infect Immun. 2007 Oct;75(10):5043–51.

116. Queen J, Satchell KJF. Neutrophils Are Essential for Containment of Vibrio cholerae to the Intestine during the Proinflammatory Phase of Infection. Infect Immun. 2012 Aug;80(8):2905–13.

117. Ritchie JM, Rui H, Bronson RT, Waldor MK. Back to the Future: Studying Cholera Pathogenesis Using Infant Rabbits. mBio. 2010 May 18;1(1):e00047-10.

118. Runft DL, Mitchell KC, Abuaita BH, Allen JP, Bajer S, Ginsburg K, et al. Zebrafish as a Natural Host Model for Vibrio cholerae Colonization and Transmission. Appl Environ Microbiol. 2014 Mar;80(5):1710–7.

119. Nag D, Farr DA, Walton MG, Withey JH. Zebrafish Models for Pathogenic Vibrios. J Bacteriol. 2020 Nov 19;202(24):e00165-20.

120. Senderovich Y, Izhaki I, Halpern M. Fish as Reservoirs and Vectors of Vibrio cholerae. PLoS ONE. 2010 Jan 6;5(1):e8607.

121. Halpern M, Izhaki I. Fish as Hosts of Vibrio cholerae. Front Microbiol. 2017 Feb 28;8:282.

122. Nag D, Mitchell K, Breen P, Withey JH. Quantifying Vibrio cholerae Colonization and Diarrhea in the Adult Zebrafish Model. J Vis Exp JoVE. 2018 Jul 12;(137):57767.

123. Wallace KN, Akhter S, Smith EM, Lorent K, Pack M. Intestinal growth and differentiation in zebrafish. Mech Dev. 2005 Feb 1;122(2):157–73.

124. Flores EM, Nguyen AT, Odem MA, Eisenhoffer GT, Krachler AM. The Zebrafish as a Model for Gastrointestinal Tract - Microbe Interactions. Cell Microbiol. 2020 Mar;22(3):e13152.

125. Willms RJ, Foley E. Mechanisms of epithelial growth and development in the zebrafish intestine. Biochem Soc Trans. 2023 Jun 9;51(3):1213–24.

126. Jones LO, Willms RJ, Xu X, Graham RDV, Eklund M, Shin M, et al. Single cell resolution of the adult zebrafish intestine under conventional conditions, and in response to an acute vibrio cholerae infection. 2023 Apr 15; Available from: http://biorxiv.org/lookup/doi/10.1101/2023.04.14.536919

127. Davoodi S, Foley E. Host-Microbe-Pathogen Interactions: A Review of Vibrio cholerae Pathogenesis in Drosophila. Front Immunol. 2020;10.

128. Blow NS, Salomon RN, Garrity K, Reveillaud I, Kopin A, Jackson FR, et al. Vibrio cholerae Infection of Drosophila melanogaster Mimics the Human Disease Cholera. PLoS Pathog. 2005 Sep;1(1):e8.

129. Anderson AML, Varkey JB, Petti CA, Liddle RA, Frothingham R, Woods CW. Non-o1 Vibrio cholerae septicemia: Case report, discussion of literature, and relevance to bioterrorism. Diagn Microbiol Infect Dis. 2004 Aug 1;49(4):295–7.

130. Purdy AE, Watnick PI. Spatially selective colonization of the arthropod intestine through activation of Vibrio cholerae biofilm formation. Proc Natl Acad Sci. 2011 Dec 6;108(49):19737–42.

131. Guichard A, Cruz-Moreno B, Aguilar B, van Sorge NM, Kuang J, Kurkciyan AA, et al. Cholera Toxin Disrupts Barrier Function by Inhibiting Exocyst-Mediated Trafficking of Host Proteins to Intestinal Cell Junctions. Cell Host Microbe. 2013 Sep 11;14(3):294–305.

132. Avadhanula V, Weasner BP, Hardy GG, Kumar JP, Hardy RW. A Novel System for the Launch of Alphavirus RNA Synthesis Reveals a Role for the Imd Pathway in Arthropod Antiviral Response. PLOS Pathog. 2009 Sep 18;5(9):e1000582.

133. Ferreiro MJ, Pérez C, Marchesano M, Ruiz S, Caputi A, Aguilera P, et al. Drosophila melanogaster White Mutant w1118 Undergo Retinal Degeneration. Front Neurosci. 2018;11.

134. Broderick NA, Buchon N, Lemaitre B. Microbiota-Induced Changes in Drosophila melanogaster Host Gene Expression and Gut Morphology. mBio. 2014 May 27;5(3):e01117-14.

135. Múnera JO, Sundaram N, Rankin SA, Hill D, Watson C, Mahe M, et al. Differentiation of Human Pluripotent Stem Cells into Colonic Organoids via Transient Activation of BMP Signaling. Cell Stem Cell. 2017 Jul 6;21(1):51-64.e6.

136. Vodovar N, Vinals M, Liehl P, Basset A, Degrouard J, Spellman P, et al. Drosophila host defense after oral infection by an entomopathogenic Pseudomonas species. Proc Natl Acad Sci U S A. 2005 Aug 9;102(32):11414–9.

137. Liehl P, Blight M, Vodovar N, Boccard F, Lemaitre B. Prevalence of Local Immune Response against Oral Infection in a Drosophila/Pseudomonas Infection Model. PLoS Pathog. 2006 Jun;2(6):e56.

138. Nehme NT, Liégeois S, Kele B, Giammarinaro P, Pradel E, Hoffmann JA, et al. A Model of Bacterial Intestinal Infections in Drosophila melanogaster. PLoS Pathog. 2007 Nov;3(11):e173.

139. Leulier F, Parquet C, Pili-Floury S, Ryu JH, Caroff M, Lee WJ, et al. The Drosophila immune system detects bacteria through specific peptidoglycan recognition. Nat Immunol. 2003 May;4(5):478–84.

140. Werner T, Borge-Renberg K, Mellroth P, Steiner H, Hultmark D. Functional Diversity of the Drosophila PGRP-LC Gene Cluster in the Response to Lipopolysaccharide and Peptidoglycan*. J Biol Chem. 2003 Jul 18;278(29):26319–22.

141. Kaneko T, Goldman WE, Mellroth P, Steiner H, Fukase K, Kusumoto S, et al. Monomeric and Polymeric Gram-Negative Peptidoglycan but Not Purified LPS Stimulate the Drosophila IMD Pathway. Immunity. 2004 May 1;20(5):637–49.

142. Stenbak CR, Ryu JH, Leulier F, Pili-Floury S, Parquet C, Hervé M, et al. Peptidoglycan Molecular Requirements Allowing Detection by the Drosophila Immune Deficiency Pathway1. J Immunol. 2004 Dec 15;173(12):7339–48.

143. Takehana A, Yano T, Mita S, Kotani A, Oshima Y, Kurata S. Peptidoglycan recognition protein (PGRP)-LE and PGRP-LC act synergistically in Drosophila immunity. EMBO J. 2004 Nov 24;23(23):4690–700.

144. Bosco-Drayon V, Poidevin M, Boneca IG, Narbonne-Reveau K, Royet J, Charroux B. Peptidoglycan Sensing by the Receptor PGRP-LE in the Drosophila Gut Induces Immune Responses to Infectious Bacteria and Tolerance to Microbiota. Cell Host Microbe. 2012 Aug 16;12(2):153–65.

145. Kamareddine L, Robins WP, Berkey CD, Mekalanos JJ, Watnick PI. The Drosophila Immune Deficiency Pathway Modulates Enteroendocrine Function and Host Metabolism. Cell Metab. 2018 Sep 4;28(3):449-462.e5.

146. Chou S, Bui NK, Russell AB, Lexa KW, Gardiner TE, LeRoux M, et al. Structure of a Peptidoglycan Amidase Effector Targeted to Gram-Negative Bacteria by the Type VI Secretion System. Cell Rep. 2012 Jun 28;1(6):656–64.

147. Le NH, Pinedo V, Lopez J, Cava F, Feldman MF. Killing of Gram-negative and Gram-positive bacteria by a bifunctional cell wall-targeting T6SS effector. Proc Natl Acad Sci. 2021 Oct 5;118(40):e2106555118.

148. Crisan CV, Chande AT, Williams K, Raghuram V, Rishishwar L, Steinbach G, et al. Analysis of Vibrio cholerae genomes identifies new type VI secretion system gene clusters. Genome Biol. 2019 Aug 12;20:163.

149. Dutta D, Dobson AJ, Houtz PL, Gläßer C, Revah J, Korzelius J, et al. Regional Cell-Specific Transcriptome Mapping Reveals Regulatory Complexity in the Adult Drosophila Midgut. Cell Rep. 2015 Jul 14;12(2):346–58.

150. Zhai Z, Boquete JP, Lemaitre B. Cell-Specific Imd-NF-κB Responses Enable Simultaneous Antibacterial Immunity and Intestinal Epithelial Cell Shedding upon Bacterial Infection. Immunity. 2018 May;48(5):897-910.e7.

151. Huang RL, Yuan Y, Zou GM, Liu G, Tu J, Li Q. LPS-Stimulated Inflammatory Environment Inhibits BMP-2-Induced Osteoblastic Differentiation Through Crosstalk Between TLR4/MyD88/NF-κB and BMP/Smad Signaling. Stem Cells Dev. 2014 Feb;23(3):277–89.

152. Feng JQ, Xing L, Zhang JH, Zhao M, Horn D, Chan J, et al. NF-κB Specifically Activates BMP-2 Gene Expression in Growth Plate Chondrocytes in Vivo and in a Chondrocyte Cell Line in Vitro *. J Biol Chem. 2003 Aug 1;278(31):29130–5.

153. Graham TR, Odero-Marah VA, Chung LW, Agrawal KC, Davis R, Abdel-Mageed AB. PI3K/Akt-Dependent Transcriptional Regulation and Activation of BMP-2-Smad Signaling by NF-κB in Metastatic Prostate Cancer Cells. The Prostate. 2009 Feb 1;69(2):168–80.

154. Tian A, Jiang J. Intestinal epithelium-derived BMP controls stem cell self-renewal in Drosophila adult midgut. Banerjee U, editor. eLife. 2014 Mar 11;3:e01857.

155. Li Z, Zhang Y, Han L, Shi L, Lin X. Trachea-Derived Dpp Controls Adult Midgut Homeostasis in Drosophila. Dev Cell. 2013 Jan 28;24(2):133–43.

156. Tian Q, He XC, Hood L, Li L. Bridging the BMP and Wnt Pathways by PI3 Kinase/Akt and 14-3-3? Cell Cycle. 2005 Feb 19;4(2):218–9.

157. Kim BG, Li C, Qiao W, Mamura M, Kasperczak B, Anver M, et al. Smad4 signalling in T cells is required for suppression of gastrointestinal cancer. Nature. 2006 Jun;441(7096):1015–9.

158. Boehm T, Bleul CC, Schorpp M. Genetic dissection of thymus development in mouse and zebrafish. Immunol Rev. 2003 Oct;195:15–27.

159. Lewis KL, Del Cid N, Traver D. Perspectives on antigen presenting cells in zebrafish. Dev Comp Immunol. 2014 Sep;46(1):63–73.

160. Zhu L yun, Lin A fu, Shao T, Nie L, Dong W ren, Xiang L xin, et al. B Cells in Teleost Fish Act as Pivotal Initiating APCs in Priming Adaptive Immunity: An Evolutionary Perspective on the Origin of the B-1 Cell Subset and B7 Molecules. J Immunol. 2014 Mar 15;192(6):2699–714.

161. Brugman S. The zebrafish as a model to study intestinal inflammation. Dev Comp Immunol. 2016 Nov 1;64:82–92.

162. Jung HM, Castranova D, Swift MR, Pham VN, Venero Galanternik M, Isogai S, et al. Development of the larval lymphatic system in zebrafish. Dev Camb Engl. 2017 Jun 1;144(11):2070–81.

163. Willms RJ, Jones LO, Hocking JC, Foley E. A cell atlas of microbe-responsive processes in the zebrafish intestine. Cell Rep. 2022 Feb 1;38(5):110311.

164. Means AL, Freeman TJ, Zhu J, Woodbury LG, Marincola-Smith P, Wu C, et al. Epithelial Smad4 Deletion Up-Regulates Inflammation and Promotes Inflammation-Associated Cancer. Cell Mol Gastroenterol Hepatol. 2018 May 24;6(3):257–76.

165. Lindholm HT, Parmar N, Drurey C, Campillo Poveda M, Vornewald PM, Ostrop J, et al. BMP signaling in the intestinal epithelium drives a critical feedback loop to restrain IL-13–driven tuft cell hyperplasia. Sci Immunol. 2022 May 13;7(71):eabl6543.

166. Liu L, Wang Y, Yu S, Liu H, Li Y, Hua S, et al. Transforming Growth Factor Beta Promotes Inflammation and Tumorigenesis in Smad4-Deficient Intestinal Epithelium in a YAP-Dependent Manner. Adv Sci. 2023 Jun 1;10(23):2300708.

167. Waaij DV der, Vries JMB de, Wees JECL van der. Colonization resistance of the digestive tract in conventional and antibiotic-treated mice. Epidemiol Infect. 1971 Sep;69(3):405–11.

168. Breen P, Winters AD, Theis KR, Withey JH. The Vibrio cholerae Type Six Secretion System Is Dispensable for Colonization but Affects Pathogenesis and the Structure of Zebrafish Intestinal Microbiome. Infect Immun. 89(9):e00151-21.

169. Pasetti MF, Levine MM. Insights from Natural Infection-Derived Immunity to Cholera Instruct Vaccine Efforts. Clin Vaccine Immunol CVI. 2012 Nov;19(11):1707–11.

170. Harris AM, Bhuiyan MS, Chowdhury F, Khan AI, Hossain A, Kendall EA, et al. Antigen-Specific Memory B-Cell Responses to Vibrio cholerae O1 Infection in Bangladesh. Infect Immun. 2009 Sep;77(9):3850–6.

171. Qadri F, Ryan ET, Faruque ASG, Ahmed F, Khan AI, Islam MM, et al. Antigen-specific immunoglobulin A antibodies secreted from circulating B cells are an effective marker for recent local immune responses in patients with cholera: comparison to antibody-secreting cell responses and other immunological markers. Infect Immun. 2003 Aug;71(8):4808–14.

172. Alavi S, Mitchell JD, Cho JY, Liu R, Macbeth JC, Hsiao A. Interpersonal Gut Microbiome Variation Drives Susceptibility and Resistance to Cholera Infection. Cell. 2020 Jun 25;181(7):1533-1546.e13.

173. Hsiao A, Shamsir Ahmed AM, Subramanian S, Griffin NW, Drewry LL, Petri WA, et al. Members of the human gut microbiota involved in recovery from Vibrio cholerae infection. Nature. 2014 Nov 20;515(7527):423–6.

174. Abby SS, Cury J, Guglielmini J, Néron B, Touchon M, Rocha EPC. Identification of protein secretion systems in bacterial genomes. Sci Rep. 2016 Mar 16;6(1):23080.

175. Kostiuk B, Unterweger D, Provenzano E, Pukatzki S. T6SS intraspecific competition orchestrates Vibrio cholerae genotypic diversity. Int Microbiol Off J Span Soc Microbiol. 2017;(20):130–7.

176. Alcoforado Diniz J, Coulthurst SJ. Intraspecies Competition in Serratia marcescens Is Mediated by Type VI-Secreted Rhs Effectors and a Conserved Effector-Associated Accessory Protein. J Bacteriol. 2015 Jun 19;197(14):2350–60.